Published in final edited form as:
J Am Chem Soc. 2021 February 03; 143(4): 1699–1721. doi:10.1021/jacs.0c12816.

Main Group Redox Catalysis of Organopnictogens: Vertical Periodic Trends and Emerging Opportunities in Group 15

Jeffrey M. Lipshultz[†], **Gen Li**[†], **Alexander T. Radosevich**
Department of Chemistry, Massachusetts Institute of Technology, Cambridge, MA, 02139, United States

Abstract

A growing number of organopnictogen redox catalytic methods have emerged–especially within the past ten years–that leverage the plentiful reversible two-electron redox chemistry within group 15. The goal of this *Perspective* is to provide the context to understand the dramatic developments in organopnictogen catalysis over the past decade with an eye towards future development. An exposition of the fundamental differences in the atomic structure and bonding of the pnictogens, and thus the molecular electronic structure of organopnictogen compounds, is presented to establish the backdrop against which organopnictogen redox reactivity–and ultimately catalysis–is framed. A deep appreciation of these underlying periodic principles informs an understanding of the differing modes of organopnictogen redox catalysis and evokes the key challenges to the field moving forward. We close by addressing forward-looking directions likely to animate this area in the years to come. What new catalytic manifolds can be developed through creative catalyst and reaction design that take advantage of the intrinsic redox reactivity of the pnictogens to drive new discoveries in catalysis?

Graphical Abstract

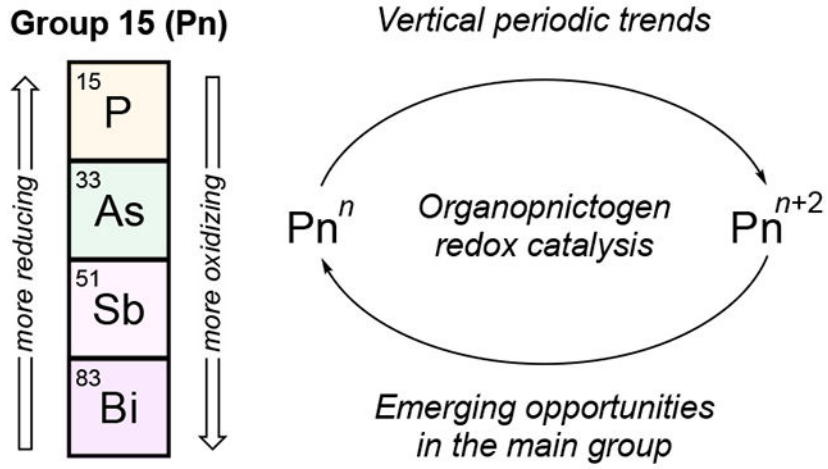

Corresponding Author **Alexander T. Radosevich** – radosevich@mit.edu.
[†]J.M.L. and G.L. contributed equally to the manuscript.

The authors declare no competing financial interest.

1. Introduction

Chemistry is patterned by elemental properties arising from the quantum structure of atoms.[1] As systematized in the periodic table, an element's periodic position corresponds with approximate expectations about its properties.[2] Accordingly, the redox reactivity of the elements is usefully (even if somewhat over-simplistically) abstracted according to their periodic 'block'. For elements in the *s*- and *f*-blocks, single oxidation states[3] (+I or +II for *s* elements,[4-6] +III for *f* elements[7,8]) tend to prevail; by contrast, numerous stable oxidation states separated by modest reduction potentials proliferate among the transition metals of the *d*-block.[9] Especially for the late transition metals of the second (4*d*) and third row (5*d*), the prevalence of accessible two-electron redox processes provides the thermodynamic and mechanistic basis[10] upon which innumerable groundbreaking discoveries in catalytic synthesis are built.[11-14]

The elements of the *p*-block—especially the 'heavier' entrants of principle quantum number $n \geq 3$—are more akin to their neighbors in the *d*-block than they are to either the *s*- or *f*-blocks in terms of breadth of accessible oxidation states. Representatively, compounds of the group 15 elements (collectively known as the pnictogens,[15,16] abbreviated Pn) express a rich redox reactivity,[17-20] where the valence electronic ns^2np^3 configuration gives rise to compounds that span −III to +V oxidation states.[21-25]

Correspondingly, discrete chemical reactions involving redox events at pnictogen centers have been described since at least the early 19th century.[26,27] Since that time, many developments in the synthetic chemistry of organopnictogen-based two-electron redox are intimately connected to pioneering achievements of 20th century organic chemistry. Staudinger's reduction of organic azides by P(III) reagents to give P(V) iminophosphoranes is a bedrock reaction in organic synthesis[28-30] that continues to find new applications in catalysis[31-33] and chemical biology.[34-39] Wittig's olefin synthesis,[40-42] which leverages the driving force $P^{III} \rightarrow P^{V}=O$, ushered in a new era in industrial preparation of carotenoids, such as vitamin A.[43] Further down group 15, unique aryl transfer reagents were introduced by Barton based on the conversion $Bi^{V} \rightarrow Bi^{III}$,[44-46] a forerunner to ongoing oxidative organopnictogen method development. In short, the impact of organopnictogen-based redox methods on synthesis is both long and celebrated.

New developments that merge elementary organopnictogen redox reactions into catalytic cycles involving formal two-electron redox cycling have been gathering pace, especially within the past decade. These developments, proceeding in parallel with ongoing synthetic redox method developments elsewhere in the *p*-block in Groups 13,[47-50] 14,[51,52] 16,[53-58] and 17,[59-68] represent the vanguard of a new class of redox catalysts composed of main group elements that evoke an analogy with well-established activation modes of the late *d*-block elements.[69-74]

Along with ample fundamental science motivations, the attractiveness of redox catalysts derived from the heavier group 15 elements is buoyed in a practical sense by the relative abundance and low cost of these pnictogens.[75] Phosphorus is abundant both in the earth's crust (1300 ppm) and in the biosphere, being the only member of the pnictogen family other

than nitrogen that is essential to life. While the heavier pnictogens are comparatively more scarce (As, 5.7 ppm; Sb, 0.75 ppm; Bi, 0.23 ppm), all are produced on >20,000 ton scale annually.[76] And though bismuth is only roughly as abundant terrestrially as palladium (0.52 ppm) and platinum (0.5 ppm), it is 10^3–10^4 times less expensive on a per kilogram basis (cf. $7.50/kg for Bi, ~$75000/kg for Pd, ~$33000/kg for Pt). Indeed, established non-redox activation modes in organopnictogen catalysis (i.e. Lewis acid,[77-79] Lewis base,[80-82] and frustrated Lewis pair[83-86] catalysis), along with the long history of Group 15 compounds as supporting ligands in organometallic chemistry,[87-94] serve as a validation of the viability of organopnictogens as constituents of practical catalysts.

In this *Perspective*, we wish to highlight exciting recent advances in the burgeoning field of organopnictogen redox catalysis. Our major goals are: (1) to identify the pivotal contributions defining the current state of the art and (2) to articulate future directions that are likely to define the forefront of research moving forward. Toward these goals, we first trace the fundamental periodic properties of the group 15 elements and then illustrate how these periodic trends are expressed in the diversity of reactions driven by group 15 redox catalysis. In this way, we hope to convey not only an appreciation of the new synthetic capabilities revealed by group 15 redox catalysis, but also a context for understanding of the relationships—both similarities and distinctions—between the congeneric elements in terms of their catalytic chemistry. By conceptualizing group 15 redox catalysis in this way as a worthy catalytic modality, we hope that this *Perspective* will knit together the broad cross-section of synthetic inorganic and organic chemists active in the organopnictogen area and serve to nucleate new efforts in this productive and promising area of research.

2. Periodicity and Vertical Trends in Group 15

Given that an informed understanding of the periodic trends and the related structural, bonding, and electronic features of organopnictogens establishes the guiding principles for further development of this field of catalysis, the purpose of this section is to provide a targeted evaluation of key features of the elements themselves and organic molecules containing them that drive the redox catalytic reactivity endemic to each pnictogen. Interested readers can find further elaboration of many of these themes in prior monographs and reviews.[95-100]

2.1 Trends in Atomic Electronic Structure.

The importance of atomic electronic structure in chemical bonding and reactivity is an essential feature of molecular orbital theory. As expanded below, the relative importance of *s* and *p* valence atomic functions in organopnictogen bonding and molecular structure—and thus reactivity— varies intrinsically with spatial and energetic atomic orbital disposition.

2.1.1 Valence orbital size.—A graph of the radial probability maxima for the valence *s* and *p* orbitals of the group 15 elements is given in Figure 1A.[101] As expected for the increasing principal quantum number, the radial extension of the valence AOs increases down the group, but three subtleties of the periodic atomic electronic structure are noteworthy. First, the increase in size—though monotonic—is not smooth. Instead, a ‘sawtooth’ shape is evident, such that the van der Waals radii of P (1.80 Å) and As (1.85 Å)

are clustered, as are Sb (2.05 Å) and Bi (2.07 Å). This effect has been attributed to a 'secondary periodicity'[102,103] arising from incomplete screening of nuclear charge owing to the intervention of the *d*- and *f*-elements on period 4 (As) and 6 (Bi), respectively (i.e. the 'scandide' and 'lanthanide' contractions).[104] Second, the increase in radial extension does not affect *s* and *p* orbitals equivalently.[105] For valence 2s and 2p orbitals of nitrogen, the probability maximum in the radial distribution function is nearly identical (0.54 and 0.52 Å, respectively), but for the 3s and 3p orbitals of phosphorus it differs by ca. 15%. The radial differences between n*s* and n*p* are even more pronounced for As, Sb, and Bi. This phenomenon arises because the 2p orbital lacks a core shell of the same angular momentum (l=1) and thus does not have a radial node, whereas radial nodes are requisite for all *p* orbitals of higher principal quantum number (n>2) to satisfy quantum orthogonality. In effect, the first-filled *p* orbital shell exerts an outward effect on all higher *p* shells through 'primogenic repulsion,' as coined by Pyykkö.[106,107] Kaupp has further emphasized the importance of radial nodes in main group bonding and reactivity.[108,109] Third, spin-orbit coupling and relativistic effects take on significant importance for bismuth.[110-113] The $6p_{1/2}$ and $6p_{3/2}$ spinors diverge markedly in radial extension, and the 6s orbital experiences a significant contraction compared to a notional 'nonrelativistic bismuth.' The importance of these orbital effects, especially the latter, has very profound consequences for the chemical and redox reactivity of bismuth (vide infra).

2.1.2 Valence orbital ionization energies.—A plot of the valence atomic orbital one-electron ionization energies is shown in Figure 1B.[101] As seen especially for the heavier pnictogens (P—Bi), valence *p* orbital energy increases uniformly down group 15. By contrast, the *s* orbital ionization energy does not exhibit such a monotonic trend. Instead, the 'sawtooth' profile is again seen; note for instance that the magnitude of the one-electron binding energy of the As 4s orbital is slightly larger than that of the P 3s orbital and that the Bi 6s orbital ionization energy is substantially larger than that of the Sb 5s orbital. These effects can be traced back to the *d*- and *f*-block contractions,[104] which is augmented in the latter case by the relativistic stabilization of the Bi 6s orbital and spin-orbit splitting of the p½ and $p^{3}/_{2}$ orbital energies.[114]

2.2 Trends in Molecular and Electronic Structure.

2.2.1 Bonding and Hybridization.—The interplay of AO radial sizes and energies has significant effects on the bonding of the heavier pnictogens. Kutzelnigg has explained that the decreased spatial overlap of the *s* and *p* orbitals down group 15 results in less *s*/*p* mixing and a lifting of the orthogonality for *s*/*p* hybrid orbitals.[115,116] As illustrated by Kaupp for the series H_3Pn (Pn=P—Bi), valence *s*-character accumulates in the non-bonding lone-pair orbital down the group, and the Pn—H bonds tend to be made increasingly from essentially unhybridized *p*-orbitals.[109] This 'hybridization defect' arising from the increasingly disparate *s* and *p* orbital sizes generally leads to weakening of σ bond energies down group 15. Thus, for the series H_3Pn (Pn=P—Bi), a consistent decrease in the Pn—H bond dissociation enthalpy is observed down the group (P: 81.4, As: 74.6, Sb: 63.3, Bi: 51.8 kcal/mol).[117,118]

2.2.2 Tricoordination.—Data for the triphenylpnictogen(III) compounds (Ph_3Pn) in the Cambridge Structural Database[119] exemplify the periodic trend in molecular structure that trace the molecular-electronic structure nexus (Fig. 2). In accord with the trend in atomic size (Sect 2.1.1), a sawtooth-like increase in Pn—C bond lengths in the $PnPh_3$ series – PPh_3 (CSD-1238522),[120] $AsPh_3$ (CSD-1318411),[121] $SbPh_3$ (CSD-1318403),[122] $BiPh_3$ (CSD-1468789)[123] – is observed, where P—C (1.93 Å) and As—C (1.96 Å) are shorter bond lengths than Sb—C (2.15 Å) and Bi—C (2.25 Å). Relatedly, the average bond angle ∠C-Pn-C decreases down the group: ∠C-P-C 102.7°, ∠C-As-C 100.4°, ∠C-Sb-C 96.6°, and ∠C-Bi-C 93.7°. Two mutually reinforcing effects drive this trend: (1) the longer bond lengths of the heavier pnictogens ease steric crowding between the aryl substituents and thus permit narrower bond angles, and (2) the *s*/*p* hybridization defect leads to increasingly directional bonding down the group (i.e. higher *p*-orbital contribution to Pn—C bonding and greater accumulation of *s*-character in the nonbonding lone pair). The longer bond lengths and greater pyramidalization of the heavier pnictogens are common features of trigonal tricoordinate group 15. As a corollary, the barrier to pyramidal inversion of trivalent organopnictogens via the 'umbrella coordinate' increases down the group.[124,125] By transit from a pyramidal C_{3v} to a planar D_{3h} geometry, the HOMO nonbonding lone pair ($2a_1$) correlates with the atomic *p* orbital oriented along the rotational axis. The energetic penalty to planarization thus imposed, which is accentuated in the case of bismuth by the relativistic stabilization of the 6s orbital relative to the 6p set,[126] has been correlated with the electronegativity of the central pnictogen within the context of a second-order Jahn-Teller effect.[127]

As will be detailed in subsequent sections, many of the organopnictogen compounds that exhibit catalytic redox properties are nontrigonal (i.e. no local threefold symmetry).[74] The interrelation of molecular geometry and electronic structure of nontrigonal compounds can be approached by reference to the frontier correlation diagram in Figure 3. Descent from local C_{3v} symmetry by progression along the bending (*e* symmetry) normal mode gives C_s-symmetric structures. Electronically, the consequence of this symmetry-lowering distortion is a lifting of the degeneracy of the unfilled orbitals resulting in a decrease in the HOMO-LUMO energy gap. Computational and experimental validation for this electronic picture has been established for nontrigonal chelates of pnictogen(III) triamide compounds.[128-131] The ability to construct pnictogen compounds of diverse molecular shapes by appropriate constraint allows for electronic structure tailoring with profound consequences for the future of catalysis in this area.

2.2.3 Pentacoordination.—In parallel to the foregoing discussion of tricoordinate pnictogen(III) compounds, the pentaphenylpnictogen(V) compounds (Ph_5Pn) first prepared by Wittig[132-134] illustrate relevant periodic trends for molecular compounds in pentacoordination (Fig. 4). Solid state structures for Ph_5P (CSD-1232414)[135] and Ph_5As (CSD-1230863)[136] are well-described as trigonal bipyramidal (τ = 0.90 and 0.98, respectively). By contrast, the heavier congeners Ph_5Sb (CSD-1232410)[137] and Ph_5Bi (CSD-1254431)[138] crystallize as distorted square pyramidal structures (τ = 0.25 and 0.22, respectively).[139,140] These static structures provide snapshots spanning the Berry pseudorotation coordinate,[141,142] and spectroscopic evidence supports that they persist in

solution.[143] Intriguingly, whereas Ph_5P, Ph_5As, and Ph_5Sb are all colorless solids, Ph_5Bi is violet.[144,145] Seppelt and Pyykkö have provided evidence that a ligand-to-metal charge transfer excitation in the visible region results from Bi-based LUMO composed of the relativistically-stabilized 6s orbital.[146,147] Without relativistic considerations, the HOMO-LUMO gap is predicted to be 27% larger, such that "'nonrelativistic' pentaphenylbismuth would not be violet." The connection between the observed low-energy optical transition and the propensity for Ph_5Bi to react as an electrophilic aryl transfer reagent has been noted.[148]

2.3 Trends in Dative and Redox Reactivity.

2.3.1 Measures of donor reactivity.—The dissociation enthalpy for Lewis adducts with group 13 Lewis acids provides a measure of donor ability of trivalent organopnictogens.[149] On the basis of gas phase experiments with AlH_3, acid-base adduct formation is most favorable for P and least favorable for Bi (Fig, 5, left). These findings correlate with qualitative observations regarding nucleophilic reactivity; triphenylphosphine and triphenylarsine readily undergo alkylation with methyl iodide, but triphenylstibine requires the more reactive trimethyloxonium electrophile $(Me_3O)BF_4$ to undergo quaternization, while triphenylbismuth is not quaternized even with $(Me_3O)BF_4$.[150,151] However, steric effects often are entangled with this underlying trend. Specifically, the relatively small atomic radii of phosphines and arsines relative to stibines and bismuthines give rise to a substantial repulsive interaction with sterically encumbered Lewis acids ($^{i}Pr_3Pn$—$Al^{t}Bu_3$ series, Fig. 5, right), resulting in accordingly diminished energetic stabilization of the Lewis adduct. In effect, the lighter pnictogens are more sensitive to steric influences than their heavier congeners.[152-154]

2.3.2 Aqueous reduction potentials.—The standard electrode potentials for the group 15 ions in aqueous solution establish an important trend governing the redox reactivity of these elements.[155] As shown in the Frost diagram in Figure 6,[156] phosphorus is the only element for which the Pn(III) and Pn(V) oxyacids are more stable than the elemental form. These positive oxidation states become increasingly unstable down the group; high valent Bi(V) is the least stable among Pn(V) congeners. This increasing preference for the lower valent state among the heavier group 15 elements can be viewed as a manifestation of the 'inert pair effect,[98-100,157-159] which in turn may be related to the hybridization defects within the high-valent compounds.[116] Computed Pn(V)=O bond energies from the reaction $H_3Pn + 0.5O_2 \rightarrow H_3Pn{=}O$ series (MP2/DZ+d level) display a similar effect, wherein phosphorus forms the most stable oxide while bismuthine oxide is energetically uphill.[160] As such, as a general rule the Pn^{III}/Pn^{V} redox couples can be summarized as follow: P^{III}/P^{V} is strongly reducing, As^{III}/As^{V} and Sb^{III}/Sb^{V} are mildly oxidizing, and Bi^{III}/Bi^{V} is strongly oxidizing.

2.3.3 Thermodynamics of reductive elimination from 5-coordinate pnictoranes—Similarly to the relative stabilities of the pnictide oxides described above, evaluation of the relative thermodynamic stabilities PnX_5 compounds with respect to PnX_3 illuminates a periodic trend (Fig. 7). Among the PnF_5 congeners, BiF_5, which is known to fluorinate hydrocarbons,[161,162] is at least 45 kcal/mol less stable than the lighter congeners,

[163,164] such as the stable, Lewis acidic PF_5. Similarly, the PnH_5 series[165] displays an irregular thermodynamic trend for the liberation of H_2 and PnH_3, in which decomposition of BiH_5 is at least 20 kcal/mol more favorable than any of the lighter congeners, owing again to the substantially more oxidizing nature of Bi(V). As will be shown, these general characterizations manifest in markedly differing reactivity of organopnictogens, and thus provide a framework for appreciating the divergences in application in redox catalysis.

The foregoing atomic properties and molecular reactivity trends are the fundamental backdrop against which the varied organopnictogen reactivity described in this *Perspective* is brought into relief. As described below, these periodic trends govern much of the divergent structure, bonding, and electronic nature of the recently uncovered examples of organopnictogen redox catalysis.

3. State-of-the-Art Developments in Organopnictogen Redox Catalysis

Although an initial report can be traced to 1981,[166] the overwhelming majority of demonstrations in the field of organopnictogen redox catalysis have come in the past decade. In this section, the key developments will be discussed, organized first by pnictogen element and then by reaction type. The purpose of this section is to develop a systematic perspective on the state of the field, with an eye toward understanding prevailing themes and, accordingly, gaps in current knowledge which might present avenues for further research.

3.1. Organophosphorus Redox Catalysis.

As described in the preceding section, the redox chemistry of organophosphorus molecules is primarily driven by the reducing nature of the P(III) state and the relative stability of the P(V) oxidation state, especially those compounds possessing P(V)=O moieties.[167-169] As such, the oxidation of P(III) compounds to stable P(V) species can be accomplished with a variety of oxidants of even modest oxidizing power.[170-177] Conversely, the reduction of P(V) to P(III) is often contrathermodynamic, thus requiring relatively forcing conditions or bespoke molecular design;[178-182] *this presents the primary challenge* in achieving organophosphorus redox cycling.

In practice, the relatively strong P(V)=O bond typically requires strong reductants[183] such as metal hydrides to generate the P(III) species via the intermediacy of a hydridophosphorane.[184] However, the barrier to reduction is lower for constrained cyclic phosphine oxides relative to unstrained cyclic[185] or acyclic[186,187] congeners, providing a rationale for catalyst design operating in the P^{III}/P^{V}=O couple. Reductive ligand coupling represents another available avenue for the reduction of P(V) species, as described in a seminal report by Mann in 1948[188-192] and modernized into a programmable process by McNally.[193-195] Nevertheless, the poor driving force inherent to P(V) to P(III) reduction presents the key challenge in achieving self-contained organophosphorus redox cycling.

3.1.1 Catalytic Wittig Reaction.—The Wittig reaction is a cornerstone of organophosphorus chemistry, and efforts to render it catalytic in phosphine require a strategy for mild and swift reduction of the phosphine oxide byproduct to enable P^{III}/P^{V} redox cycling. The past 12 years have seen the successful application of novel organophosphorus

molecules to achieve such a feat.[196-199] In 2009, O'Brien reported the first example of organophosphorus redox catalysis using a five-membered phospholane oxide (3-methyl-1-phenylphospholane 1-oxide) **P1•[O]** operating in the P^{III}/P^{V}=O couple in the context of a Wittig reaction (Fig. 8A).[200] This strategy uses a mild hydrosilane reductant, Ph_2SiH_2, to reduce the phospholane oxide precatalyst to the active P(III) species, which can then undergo quaternization, deprotonation, and Wittig reaction to obtain the desired product olefin and regenerate the phospholane oxide pre-catalyst. In 2013, O'Brien significantly lowered the reaction temperature for catalytic Wittig reactions to ambient temperature via the use of a Bronsted acidic additive, 4-nitrobenzoic acid, which enhances the rate of reduction of phosphine oxide **P2•[O]** (Fig. 8B).[201] O'Brien further developed a series of electron-deficient phospholane oxide precatalysts, including **P3•[O],** to enable the use of non-stabilized ylides in the catalytic Wittig reaction (Fig. 8C).[202]

Other organophosphorus catalyst scaffolds have proven adept at achieving catalytic Wittig reactions. In 2019, Werner demonstrated the utility of phosphetane[203] oxide **P4•[O]**[204] to enable catalytic Wittig reaction at 1 mol% catalyst loading at ambient temperature in the absence of any acidic additive (Fig. 9).[205] Simple phosphine oxide precatalysts, such as Ph_3PO, Oct_3PO, or Bu_3PO, have been explored for catalytic Wittig reactions, but to this point have required the assistance of microwave heating or Bronsted acid additive at high temperature.[206,207]

In 2014, Werner demonstrated the first enantioselective catalytic Wittig reaction operating in a P^{III}/P^{V}=O couple, highlighting some challenges in realizing such a method (Fig. 10). In this work, a variety of chiral phosphine catalysts are applied for desymmetrization of prochiral haloketone **11** to give enantioenriched diketone **12**. The most promising result utilizes (S,S)-Me-DuPhos (**P5**), a C_2-symmetric bisphospholane,[208] with phenylsilane as the terminal reductant in dioxane via microwave heating at 150 °C, which gives 39% yield and 62% *ee*.[209,210]

The formation of the phosphorus ylide can also be achieved in the absence of base through conjugate addition to activated olefins and proton transfer, as exemplified by Werner and Lin (acrylates),[211-214] Vouturiez (ynoates),[215,216] Kwon (allenes),[217] and Lin (enones)[218] using a selection of catalysts previously described (Fig. 11A). Of particular note is an enantioselective variant enabling the synthesis of (trifluoromethyl)cyclobutenes (Fig. 11B)[219] developed by Voituriez in 2018 with Kwon's bicyclic chiral phosphine oxide HypPhos **P7•[O]**.

3.1.2 Catalytic Staudinger Reactions and Aza-Wittig.—

In 2012, van Delft and Rutjes reported the first catalytic Staudinger reaction with a dibenzophosphole catalyst **P10** and $PhSiH_3$ as reductant (Fig. 12A).[220] In contrast to iminophosphorane hydrolysis employed in the stoichiometric reaction, the catalytic reaction involves direct reduction of the P(V) iminophosphorane with $PhSiH_3$ for the formation of the amine product and regeneration of the phosphine catalyst.[221] PPh_3 (**P11**) could also be used in place of the dibenzophosphole under identical conditions, albeit with significantly prolonged reaction times. Mecinović later demonstrated an ambient temperature protocol by employing an optimized hydrosilane reductant.[222] Catalytically formed iminophosphoranes from PPh_3

(**P11**) can also be used for Staudinger amidation reactions (Fig. 12B),[223] although the precise mechanism of the redox cycle is unclear.[224-226]

Other applications of iminophosphorane intermediates in the context of P^{III}/P^{V}=O cycling include catalytic aza-Wittig[227-230] and diaza-Wittig reactions (Fig. 13A).[231] In 2018, Kwon demonstrated the first catalytic asymmetric Staudinger-aza-Wittig reaction[232,233] with high levels of stereoinduction via desymmetrization of diketones using HypPhos catalyst **P12** with the assistance of a Brønsted acid additive (Fig. 13B).[234]

3.1.3 Catalytic Appel and Mitsunobu Reactions.—

Organophosphorus catalyzed oxidation-reduction condensation reactions,[235,236] such as the Appel and Mitsunobu reactions, face challenges of reagent compatibility (between halenium/azo oxidant and hydrosilane reductant) and product stability. In 2011, Rutjes and van Delft achieved a P^{III}/P^{V}=O catalyzed Appel bromination (Fig. 14A).[185] In this transformation, diethyl bromomalonate (DEBM) is an ideal bromenium donor, showing good compatibility with hydrosilane reductants. Further, the dibenzophosphole catalyst **P10** is exclusively reactive toward the bromenium source, thus selectively generating the electrophilic bromophosponium ion, but unreactive towards the brominated products.[237,238] Recently, Werner further extended the scope to chlorination of alcohols with benzotrichloride as oxidant and trioctylphosphine (**P13**) as the catalyst (Fig. 14B).[239] Catalytic Appel conditions with PPh_3 (**P11**) can also be used to drive amide couplings between carboxylic acids and amines, as demonstrated by Mecinović in 2014 (Fig. 14C).[240] Alternatively, Denton has extensively developed redox-neutral P^{V}-mediated dehydrative halogenation reactions using Ph_3PO as catalyst with oxalyl chloride as dehydrative reagent to enable phosphine oxide/phosphonium cycling.[241-248]

Recently, an annulation of amines and carboxylic acids was described via organophosphorus-driven recursive dehydration using phosphetane catalyst **P4•[O]**, DEBM, and $PhSiH_3$ or Ph_2SiH_2 (Fig. 15).[249] In this tandem catalytic reaction, the catalytically-generated bromophosphonium first induces amide coupling and then cyclodehydration in a second catalytic turnover. To facilitate the coupling of alkyl amines, fully-substituted diethyl (methyl)bromomalonate (DEMBM) is required to suppress *N*-alkylation. These conditions enable the coupling of pharmaceuticals, such as ibuprofen, without racemization at adjacent stereocenters, as well as the synthesis of dihydroisoquinoline natural products such as dihydropapaverine. Interestingly, the use of diethyl chloromalonate as the oxidant, and thus a chlorophosphonium intermediate as the dehydrating species, results in only amide bond formation.

In 2010, O'Brien again successfully applied precatalyst **P1•[O]** in a catalytic Mitsunobu-type reaction (Fig. 16).[250] Later, Aldrich disclosed some initial efforts into recycling both phosphine oxide and the azocarboxylate reagent, by an iron-phthalocyanine catalyzed process in the presence of oxygen.[251] However, a detailed study from Taniguchi reported difficulty in reproducing both yield and enantiomeric ratio for some examples, as well as successful product formation in the absence of hydrazine catalyst. These results indicate this reaction might not undergo a true Mitsunobu process, and further study appears to be necessary.[252,253] Recently, Denton has used creative catalyst design to enable redox-neutral

P^V-based catalysis operating in a phosphine oxide/phosphonium cycle to achieve a highly successful catalytic Mitsunobu reaction.[254]

3.1.4 Catalytic Reductive O-Atom Transfer.—Owing to the strongly reducing nature of trivalent P(III) compounds, phosphines are excellent O-atom acceptors from a variety of oxygenated substrates. In 2010, Woerpel described the first P^{III}/P^V=O catalyzed reductive O-atom transfer by selective reduction of alkyl silyl peroxides to silyl ether products.[255] The overall reaction is initiated by concerted insertion of triphenylphosphine into the O—O bond. Labeling and crossover studies demonstrate that a concerted elimination/silyl transfer step is operative in generating the silyl ether products and a phosphine oxide, which could in turn be selectively reduced by a titanium(III) hydride generated *in situ*.

To expand P^{III}/P^V=O catalyzed O-atom transfer to less-oxidizing oxygenated substrates, the catalytic chemistry of a biphilic[256] phosphetane catalyst scaffold has been developed. In 2015, a phosphetane-catalyzed deoxygenative condensation reaction of α-keto esters and carboxylic acids via formal carbene insertion into the protic O—H bond of the acid was described (Fig. 17).[257] The reaction initiates by Kukhtin-Ramirez addition[258] of the P(III) phosphetane **P14** to the keto ester substrate **48**. Proton transfer from the benzoic acid followed by Arbuzov-like[259] displacement of phosphine oxide **P14•[O]** from intermediate **P14b** results in formation of α-acyloxy ester product **50.** The catalytic cycle is closed by reduction of phosphetane oxide **P14•[O]** to **P14** by the hydrosilane reductant.

The phosphetane scaffold is also effective for engaging nitro groups in O-atom transfer. Building on seminal stoichiometric work by Cadogan,[260-263] in 2017 a catalytic synthesis of indazoles and benzotriazoles from nitroimine and -azo starting materials, respectively, using **P4•[O]** as precatalyst under comparatively mild conditions was described (Fig. 18).[264]

In this transformation, DFT models implicate a [3+1] cycloaddition of P(III) species to the nitro group as the turnover-limiting step. In accord with empirical observations, the barrier to this step with a phosphetane is significantly lower in energy than with an acyclic trialkylphosphine. Distortion-interaction analysis[265] of the relevant transition structures (Fig. 19) shows that the differential barrier arises from an enhanced stabilizing interaction energy for the phosphetane rather than a diminished distortion penalty.[266-269] In effect, the contracted endocyclic C-P-C bond angle results in a low-lying LUMO, thus imbuing the phosphorus center with increased biphilic character relative to acyclic and larger phosphacyclic compounds. For comparison, a similar catalytic Cadogan transformation described by Nazaré using a larger-ring phospholene oxide precatalyst requires higher catalyst loadings and significantly longer reaction times.[270]

This approach to catalytic nitro deoxygenation has been similarly applied to C—N bond-forming reactions for the synthesis of carbazoles and indoles, as shown in Figure 20.[271] Here, oxazaphosphirane intermediate **55** was observed at low temperature as the immediate precursor to carbazole formation. DFT calculations suggest an oxazaphosphirane as the pivotal intermediate, which thermally dissociates phosphine oxide **P4•[O]** to reveal a free nitrene capable of evolving to the carbazole product via C—H amination.[272]

Given that such an oxazaphosphirane intermediate might be targeted to further reaction development via heterolytic ring opening with a Lewis acid, introduction of an arylboronic acid partner to the P^{III}/P^{V}=O catalyzed nitro deoxygenation manifold resulted in a new reductive C—N cross coupling of nitroarenes and boronic acids (Fig. 21).[273] The scope was subsequently expanded to allow the reductive coupling of nitromethane with both boronic acids and esters, providing an efficient strategy for installation of the MeHN− fragment with inexpensive and easy-to-handle nitromethane as the methylamine surrogate.[274] By virtue of the nonmetal main group-catalyzed conditions for this C—N coupling, useful chemoselectivities are observed, establishing the method as a complement to existing transition metal-catalyzed techniques. Mechanistic investigations support a pathway involving formation of the oxazaphosphirane intermediate **P4b**, followed by engagement with the boronic acid **57** to make betaine **P4c**, leading to product formation via 1,2-metallate shift. This pathway is predicted to outcompete evolution of the oxazaphosphirane to a free nitrene **60**, accounting for the excellent selectivity for intermolecular cross-coupling.[275,276] The C—N coupling event can be telescoped with subsequent ring closing events to allow for the synthesis of N-aryl heterocycles (**58**) by a cross-coupling/condensation cascade, as depicted in Figure 22.[277]

Phosphetane oxide **P4•[O]** also efficiently catalyzes deoxygenative processing of sulfonyl chlorides (including trifluoromethyl- and heteroarylsulfonyl derivatives) by O-atom transfer (Fig. 23).[278] This approach has been applied to an electrophilic sulfenylation of indoles via fleeting sulfenyl(ium) electrophilic equivalents.

3.1.5 Catalytic Hydride and Hydrogen Transfer.—

Phosphetane-based catalysts have also been shown to drive regioselective transpositive reduction of allylic bromides through the intermediacy of P(V) hydrides (Fig. 24).[279] The reaction benefits from the colocalized donor and acceptor properties of the phosphetane to achieve the necessary changes in both oxidation state and coordination number. Specifically, the reaction starts with quaternization of phosphetane **P15** by the allylic bromide. In the presence of the stoichiometric reductant $LiAlH(O\text{-}t\text{Bu})_3$, hydride is delivered directly to the phosphorus center of allylic phosphonium cation **P15a** to give a hydridophosphorane **P15b** that is observable by low temperature ^{31}P NMR spectroscopy. VT-NMR kinetics experiments and DFT calculations indicate that decomposition of pentacoordinate hydridophosphorane **P15b** to the reduction products occurs regiospecifically via a concerted 5-membered, 6-electron transition state (**P15c**). This pericylic γ-reductive elimination illustrates the unique merger of conventional organic and organometallic reactivities in catalytic chemistry of the p-block compounds.

In a conceptually complementary hydride transfer reaction, an unusual transfer hydrogenation of azobenzene with ammonia borane catalyzed by P^{III}/P^{V} cycling was developed (Fig. 25). In this work, planar compound **P16**, introduced by Arduengo,[280-282] reacts with $H_3N{\bullet}BH_3$ to give dihydridophosphorane **P16a**.[283] Dihydride **P16a** in turn serves as a reactive hydrogen donor, transferring an H_2 equivalent to a variety of electrophilic organic acceptors. The combined reactivities of **P16** as hydrogen acceptor from ammonia-borane and **P16a** as hydrogen donor to an organic substrate permit the use of this

phosphorus platform as a catalyst for transfer hydrogenation. Although alternative pathways have been suggested via DFT studies,[284-286] experimental mechanistic investigations lead to the assertion that hydrogen transfer catalysis in this case involves **P16**⇌**P16a** cycling. These results establish precedent for 'dihydride' transfer hydrogenation with a *p*-block catalyst.

3.2 Organoarsenic Redox Catalysis.

The redox reactivity of organoarsenic compounds is similar, albeit less well developed, when compared to organophosphorus congeners, as might be expected by the similar valence orbital IEs of P and As (see Fig. 2B). For instance, As(III) molecules similarly undergo oxidation to As(V) with mild oxidants,[287,288] and arsonium ylides can be generated from arsonium salts[289,290] or carbene transfer[291,292] for use in Wittig-type olefination reactions. In contrast, the As(V) oxidation state is less thermodynamically stable than P(V) (see Fig. 6), such that pentacoordinate arsoranes are known to undergo reductive elimination via ligand coupling, [293] and O-atom transfer of $R_3As{=}O + PR_3 \rightarrow R_3As + O{=}PR_3$ is both kinetically and thermodynamically accessible.[294,295]

3.2.1 Catalytic Wittig Reactions.—

Taking advantage of the favorable deoxygenation of arsine oxides by P(III) reagents, the first report of organoarsenic redox catalysis was published in 1989 by Shi and Huang who described a tributylarsine-catalyzed Wittig olefination of aldehydes with activated bromoalkanes (Fig. 26).[296] Triphenylphosphite, itself not competent to drive the direct olefination reaction, serves as a terminal O-atom acceptor by deoxygenation of the arsine oxide formed by Wittig olefination. Recently, Imoto and Naka have demonstrated the ability of an arsolane to efficiently catalyze similar transformations by $As^{III}/As^{V}{=}O$ cycling with a hydrosilane reductant at 100 °C.[297]

A second approach to arsine-catalyzed Wittig reactions involves Fe-porphyrin-catalyzed carbenoid transfer to generate the requisite arsenic ylide, as demonstrated by Tang (Fig. 27).[298,299] In an initial report from 2007, triphenylarsine (**As2**) catalyzes the olefination of aldehydes with ethyl diazoacetate in the presence of an Fe-porphyrin catalyst, where sodium dithionite is the terminal reductant enabling turnover at As. In a follow-up study in 2012, the arsine catalyst is immobilized on a polymer support to enable olefination of aldehydes and ketones with use of a soluble hydrosilane reductant, PMHS, at 110 °C to enable redox cycling of the arsine catalyst. Taken together, these reports demonstrate the utility of organoarsenic compounds in the catalytic generation of arsonium ylides for olefination and the propensity for reduction of the catalytic arsine oxides intermediates. However, concerns about toxicity and stability of the organoarsenic compounds have limited the utility of such transformations, especially as new strategies for facile turnover of phosphine oxides have emerged (see Sect 3.1.1). It remains to be seen whether there are any transformations unique to organoarsenic redox catalysis that would overcome the perceived barriers to use of As in synthesis.

3.3 Organoantimony Redox Catalysis.

As compared to both P and As, the chemistry of organoantimony compounds is distinguished by the less reducing nature of the Sb(III) oxidation state and more oxidizing nature of the Sb(V) oxidation state.[300] As such, whereas oxidation of Sb(III) species can be

accomplished by reaction with strong oxidants such as bromine, peroxides, *o*-quinones, and iodoso compounds, stibines do not typically undergo quaternization with alkyl halides or Michael acceptors.[301] Conversely, the lower stability of the Sb(V) compounds results in enhanced oxidizing power in relation to the lighter pnictogens, as depicted in Fig. 9. Consequently, oxidative transformations of substrates, such as alcohol oxidation, have been described using Sb(V) compounds.[302] These stoichiometric reactions have been translated to a limited set of organoantimony-catalyzed methods.

3.3.1 Catalytic Oxidation Reactions.—

Organoantimony redox catalysis is characterized by a conspicuous opportunity for further development. At present, only two publications have appeared in this area, each of which describes an identical overall transformation under slightly modified conditions, depicted in Figure 28. In 1982, Akiba translated a stoichiometric triphenylantimony dibromide-mediated oxidation of α-hydroxyketones to α-diketones into a catalytic protocol, employing as little as 10 mol% of the Sb(V) catalyst.[303] Upon single turnover, the resultant reducing Ph_3Sb (**Sb2**) can be oxidized by the exogenous bromine surrogate 2,3-dibromo-3-phenylpropionate to regenerate the oxidizing Sb(V) dibromide (**Sb1**), turning over the cycle. 20 years later, Kurita described a more practical implementation, in which 10 mol% triphenylstibine (**Sb2**) is used directly as catalyst under aerobic oxidation conditions to effect the same transformation in nearly quantitative yield.[304]

In contrast to this mild, efficient reaction with $SbPh_3$, the use of stoichiometric PPh_3 or $BiPh_3$ both provide no benzil product (**81**), owing to chemical inertness of the P(V) and Bi(III) states, respectively. In fact, this catalytic oxidation represents the microscopic reverse of well-established P(III)-mediated 1,2-dicarbonyl reduction by Kukhtin-Ramirez addition.[305-308] Further, reaction employing $AsPh_3$ (**As2**) under air is sluggish and poorly efficient, demonstrating the varied reactivity of congeneric organopnictogens, which are each best suited to particular applications. However, this approach to catalytic alcohol oxidation via organoantimony catalysis has never been extended beyond these activated α-hydroxyketones.

3.4. Organobismuth Redox Catalysis.

The redox chemistry of the Bi^{III}/Bi^{V} couple is dominated by the manifestation of the inert pair effect.[98-100,157,158] Owing to the poor spatial and energetic overlap of Bi valence *s* and *p* orbitals,[108-109,115-116] with drastic relativistic effects of the heavy atom nucleus, only very strong oxidants can convert a Bi(III) center to Bi(V); accordingly $BiCl_3$ does not yield $BiCl_5$ upon exposure to chlorine.[309] However, Bi(V) species, such as $Ph_3Bi(OAc)_2$, are accessible through oxidation with peroxides, for example, and have been used extensively as strong oxidants, such as in alcohol oxidation, olefin oxidation, and oxidative cleavage of diols.[310,311] Further, the strongly oxidizing nature of Bi(V) centers has resulted in the development of ligand coupling reactions utilizing triaryl Bi(V) reagents, e.g. in the arylation of phenols.[44-46] Recently, these principles have been applied by Ball to programmed, stoichiometric *o*-arylation of phenols by arylboronic acids via the intermediacy of triaryl Bi(V) species.[312]

The Bi^{I}/Bi^{III} couple has been much less studied in the context of organopnictogen chemistry, as only recently have discrete redox events in this manifold been explored. Of particular note is the seminal work of Dostál, who has demonstrated that Lewis base-stabilized aryl-Bi(III) dihydrides undergo facile release of H_2 to generate the corresponding aryl-Bi(I) compounds,[313,314] which are then amenable to oxidative addition to deliver Bi(III) species.[315-317] Bismuth(III) alkoxides also undergo Bi—O homolysis in certain cases,[318-319] a potentially relevant step in the SOHIO ammoxidation process for the synthesis of acrylonitrile from propylene.[320-322] These rare examples represent the early stages of accessing low-valent organobismuth centers to enable redox events and have begun to find application in catalysis.

3.4.1 Catalytic Oxidation Reactions.—Much of the pioneering synthetic method development using organobismuth molecules can be attributed to Barton and coworkers. Indeed, the very first demonstration of any organopnictogen exhibiting redox catalysis was reported by Barton and Motherwell in 1981 (Fig. 29),[166] in which triphenylbismuth (**Bi1**) catalyzes oxidative cleavage of α-glycols using a stoichiometric oxidant such as *tert*-butyl hydrogen peroxide (TBHP) or *N*-bromosuccinimide (NBS). This discovery was predicated upon the observation that, in the stoichiometric variant using triphenylbismuth carbonate as the oxidant, quantitative conversion to triphenylbismuth (**Bi1**) is observed. As such, simply by slow addition of an exogenous oxidant to regenerate a Bi(V) species, catalytic turnover can be achieved with catalyst loadings as low as 1%. Similar reactivity of both *cis*- and *trans*-decalin-9,10-diols suggests an open intermediate enabling the oxidative cleavage, as opposed to a cyclic intermediate as has been invoked for Criegee, Malaprade, and related oxidations.[323] Here, it is relevant to note the difference in reactivity as exhibited in the $SbPh_3$-catalyzed oxidation of benzoins as described in section 3.3.1, which is limited to more activated substrates.[304]

Postel and Duñach later described a series of oxidative cleavage reactions catalyzed by Bi(III) mandelate, under molecular oxygen in DMSO.[324,325] Here, epoxides can be oxidized *in situ* to α-diketones, which are further oxidatively converted to two equivalents of carboxylic acid. Related reactions point to a dual Lewis acidic and redox role for Bi(III) in these reactions.[326-329] Other Bi(III)-catalyzed oxidation reactions, including benzylic and allylic hydroxylation with TBHP, have been reported; however, mechanistic evidence is not supportive of a Bi-redox cycle.[330-332]

3.4.2 One-electron redox via open shell intermediates.—The first demonstration of radical-mediated organobismuth catalytic reactivity was described by Coles in the context of oxidative coupling of TEMPO with phenylsilane with release of H_2 (Fig. 30).[333] In this reaction, the isolable Bi(II) radical catalyst **Bi2** can reversibly bond to TEMPO (**85**) to generate metastable Bi(III)-TEMPOxide **Bi2a**, which is proposed to undergo metathesis with a Si—H bond, generating the TEMPO—Si bonded product and Bi(III)-hydride **Bi2b**. This species was previously shown stoichiometrically to undergo oxidative loss of hydrogen, thus regenerating Bi(III) catalyst **Bi2**.[318,319] Similar catalytic reactivity was recently demonstrated by Lichtenberg using a diaryl(bismuth)thiolate catalyst under UV irradiation.[334]

3.4.2 Catalytic Cross-Coupling.—While Bi(III) and Bi(V) reagents have been used as organometallic nucleophiles and electrophiles, respectively, in transition metal-catalyzed cross couplings for more than 20 years,[335] Bi-catalyzed redox cross-coupling reactions have only recently been reported. A transition metal-like cross-coupling reaction catalyzed by two electron-processes at a Bi center was described by Cornella in 2020 (Fig. 31).[336] In this work, tethered Lewis base-supported Bi(III)-bismuthane catalyst **Bi3** undergoes transmetalation with an aryl boronic ester to generate triarylbismuthane **Bi3a**. Then, oxidation by strongly oxidizing fluoropyridinium reagent **91** yields Bi(V) species **Bi3b**, which is stabilized by the pendant Lewis basic sulfoximine. Finally, reductive elimination forges the new C—F bond of product **88** and regenerate Bi(III) species **Bi3**, turning over the cycle. This chemistry takes advantage of a tethered biaryl sulfoximine ligand framework on Bi to both stabilize highly oxidizing Bi(V) intermediates with the pendant Lewis base and yield selective ligand coupling of the exocyclic aryl ligand with the apical fluoride substituent. As described in a follow-up report, perfluoroalkyl sulfonate salts are successfully coupled using bis-CF_3 bismuthane **Bi4** bearing a sulfone tether to provide aryl triflate and nonaflate products.[337] In this catalytic platform, rational ligand design to optimize geometric and electronic properties at the central pnictogen atom serve to unveil novel, transition metal-like reactivity.

3.4.3 Catalytic Reductive Deoxygenation.—Cornella has also explored the Bi^{I}/Bi^{III} couple for catalysis in the context of transfer hydrogenation of azoarenes and nitroarenes (Fig. 32).[338] Using an NCN-chelated bismuthinidene (**Bi5**) first described by Dostál,[313,314] an unstable Bi(III)-dihydride (**Bi5a**) is putatively formed by reaction with ammonia borane, in reverse analogy to the loss of H_2 from a Bi(III)-dihydride (**Bi5a**) originally described by Dostál. In this catalytic reaction, the putative Bi(III)-dihydride (**Bi5a**) intermediate delivers H_2 across either N—N or N—O π-bonds, accomplishing a transfer hydrogenation with good functional group tolerance. Mechanistic studies support the intermediacy of the Bi(III)-dihydride (**Bi5a**), as its protonated cation (**Bi5b**) can be detected by HRMS in both stoichiometric and catalytic reactions. Here, the Bi^{I}/Bi^{III} cycle is exploited to first receive an equivalent of H_2 from ammonia borane and then deliver it to an activated π substrate, similarly to earlier work carried out in the P^{III}/P^{V} couple.[283] This reaction is the first demonstration of organopnictogen catalysis operating in the Pn^{I}/Pn^{III} couple, thus paving the way for low-valent organopnictogen chemistry in catalysis.

Cornella further demonstrated the catalytic utility of the Bi^{I}/Bi^{III} couple of bismuthinidenes such as **Bi5-Bi7** for the reductive deoxygenation of N_2O, through a distinct mechanistic pathway (Fig. 33).[339] In this study, rapid deoxygenation of N_2O by **Bi5** liberates N_2 and produces a dimeric [Bi_2O_2] species as detected by ESI-HRMS. Through careful tuning of the pendant imine ligands, aldimine-supported **Bi6** and ketimine-supported **Bi7** yield dimeric [Bi_2O_2] and monomeric [Bi—OH] scaffolds, respectively, upon exposure to N_2O, with the structures unambiguously identified by single crystal X-ray crystallography. These results seemingly indicate an unstable, basic Bi^{III}-oxide intermediate derived from O-atom transfer from N_2O. Both aforementioned oxide-derived adducts yield parent compounds **Bi6** and **Bi7**, along with HOBpin and $O(Bpin)_2$, upon exposure to HBpin at ambient temperature. Accordingly, catalytic reduction of N_2O is feasible using **Bi5**, **Bi6**, and **Bi7**,

with **Bi5** delivering the most rapid and efficient conversion, even at catalyst loadings as low as 0.1 mol%. This demonstration of Bi^{I}/Bi^{III} catalysis combines the reducing nature of the Bi(I) state with a facile reduction of a Bi(III) oxide equivalent to enable redox cycling at ambient temperature, evocative of the body of work in P^{III}/P^{V}=O redox catalysis.

4. Outlook

The quickening pace of progress in organopnictogen redox catalysis within the past fifteen years assures the continued vibrancy of this exciting area of research in the years to come. Looking ahead, we anticipate significant opportunities for ongoing discovery across a broad scientific front, including:

- *Designing Catalysts with Improved Redox Leveling.* A greater mastery over precision redox tuning will be needed to enable catalysis with greater speed (turnover frequency) and greater durability (turnover number). An appreciation for the connection between catalyst composition/structure and redox driving force of elementary reaction steps will be a necessary initial step in this quest, but a further attentiveness to round-trip thermodynamics will also be needed for catalysis. Detailed mechanistic and thermochemical studies that identify kinetic bottlenecks and parasitic branching points will be essential to inform new catalyst designs that enable faster turnover at milder conditions with lower catalyst loading. In the limit, such a high level of redox mastery would enable the reversible use of a given Pn^{n}/Pn^{n+2} couple specified only by the reaction thermodynamics of the stoichiometric inputs.
- *Taming Underexplored Two-Electron Redox Couples for Catalysis.* Although periodic trends shape the innate driving forces for two-electron redox events at pnictogens (Sect. 2), novel design of organopnictogen compounds might open space for catalytic cycles operating within ‘atypical’ redox couples. As exemplified in Sect. 3, the Pn^{III}/Pn^{V} couple has been widely employed in catalysis; by contrast, the lower-valent Pn^{I}/Pn^{III} couple is still comparatively underdeveloped. Seminal work on the chemistry of Pn(I) centers have demonstrated their ability to achieve challenging bond activation reactions.[340,341] Although the generation of low-valent Pn(I) species under mild conditions poses the most immediate barrier to expansion of organopnictogen redox catalysis to the Pn^{I}/Pn^{III} couple, pioneering work from Cornella in Bi^{I}/Bi^{III} catalysis [338,339] establishes feasibility and points to further opportunities. By expanding the accessibility of diverse redox states—presumably through ligand design and substituent effects—new channels of reactivity might be made available.
- *Controlling Stereochemistry in Organopnictogen Redox Catalysis.* The pioneering achievements of Werner,[209,210] Voituriez,[219] and Kwon[234] (Sect. 3.1) establish the viability of stereochemical control within organopnictogen redox catalysis; however, new chiral organopnictogen catalysts will be needed to advance beyond these initial discoveries. For instance, it remains to be seen whether deliberate incorporation of ‘secondary sphere’ interactions can be leveraged to effect stereochemical discrimination.[33,342-346] The opportunities

and/or complexities associated with stereogenic pnictogen chirality centers and their stereochemical fluxionality—especially in pentacoordination (i.e. polytopal isomerism)[141,142]—have not yet been explored in a systematic fashion. Indeed, given challenges presented by the varying coordination numbers, geometries and valence electron counts encountered in organopnictogen redox catalysis, the emergence of new heuristics of asymmetric design may be needed.

- *Merging Organopnictogen Redox with Established Catalytic Modes.* The merger of organopnictogen redox catalysis with other enabling modes of catalysis (organocatalysis, transition metal catalysis, Bronsted acid/base catalysis, *inter alia*) could lead to the development of further powerful classes of reactions. Such catalytic cycles could be envisioned to work in tandem, cascade,[347-351] or synergistic modes,[352] owing to the mutual compatibility of each catalytic mode of molecular transformation. Such mergers could make use of the distinct reactivities inherent to the aforementioned platforms and create opportunities for unveiling novel transformations.

- *Embracing One-electron Open-shell Reactivity.* Stable covalent bonds are (mostly) two-electron constructs, but their catalytic synthesis by stepwise one-electron processes presents potentially enabling reaction channels.[353-359] Open-shell reactivity within organopnictogen catalysis is therefore ripe for development. Organopnictogen radicals and radical ions are well-known entities,[360,361] whose reactivity can be triggered by photochemistry[362-367] or electrochemistry.[368,369] Among possible scenarios, single-electron oxidation or reduction of catalytic intermediates[370-377] could unveil new reaction pathways, including selective bond activation or challenging atom transfer processes.[378-382] Alternatively, single-electron pathways could be accessed to facilitate otherwise sluggish catalytic turnover, such as electrocatalytic reduction of phosphine oxides.[383-386]

- *Beyond Homogenous Organic Reaction Media.* The development of catalytic systems that can operate in nonorganic media will be a necessity to realize a broader potential of group 15 redox catalysis in contexts beyond organic synthesis. Noting the prevalence of organopnictogen redox chemistry in chemical biology in the form of the Staudinger ligation,[34-39] the development of water-compatible reaction systems presents an appealing challenge to the growth of the field of organopnictogen redox catalysis.[387] Indeed, recent work utilizing P(V) chemistry to selectively label serine residues[388] and Bi(V) chemistry to arylate phenols[312] point to the potential of Pn(V) to enable selective bond-forming reactions. Alternatively, an adaptation of the design principles for homogeneous group 15 redox catalysis to heterogeneous catalyst development similarly presents untold prospects for discovery.

5. Concluding Remarks

To close, we return to the question posed at the end of the Abstract: “What new catalytic manifolds can be developed through creative catalyst and reaction design that take advantage

of the intrinsic redox reactivity of the pnictogens to drive new discoveries in catalysis?”[389] This is a critical question, and though a detailed answer may not be knowable except in hindsight, the contours of a reply surely can be traced in outline. Organopnictogen redox catalysis is a relatively young entrant to the science of catalysis presently populated by numerous highly successful catalytic modalities, each a towering achievement. Within this crowded context, organopnictogen redox catalysis must aspire to more than mimicry of existing techniques; it must express something authentic and inimitable. On this front, it seems likely that the most compelling opportunities presented by this emerging field—those that will maximize scientific and practical impact—will be realized through the discovery of new bond (dis)connections or functional group interconversions that are truly native to *organopnictogen redox catalysis*. We assert that the periodic trends—both within Group 15, and between Group 15 and others in the *p*-block—impart the pnictogens generally, and each of the pnictogen elements individually, with distinctive properties, providing a varied palette of components for catalyst design and reaction development. The diversity of characteristics in Group 15 position organopnictogen redox catalysis to achieve unique reaction classes that are without direct precedent or complement in the armory of catalytic synthesis. Along this trajectory, the progress achieved thus far in organopnictogen redox catalysis is but a tantalizing preamble to a future of ongoing discovery.

ACKNOWLEDGMENT

Dedicated to Prof. F. Dean Toste (UC Berkeley) on the occasion of his 50th birthday. Financial support was provided by NIH NIGMS (GM114547) and NSF (CHE-1900060). J.M.L. thanks the Camille and Henry Dreyfus Foundation for a postdoctoral fellowship in Environmental Chemistry. G.L. thanks Bristol Myers Squibb for a graduate fellowship. We extend our genuine thanks to the peer reviewers for their thorough and thoughtful comments.

REFERENCES

1. Schwerdtfeger P; Smits O; Pyykkö P The periodic table and the physics that drives it. Nat. Rev. Chem 2020, 4, 359–380.
2. Mendeleev emphasized the periodic variation in oxidation number for the then-known elements: Mendelejeff D Ueber die Beziehungen der Eigeschaften zu den Atomgewichten der Elemente (On the Relationship of the Properties of the Elements to their Atomic Weights). Z. Chem 1869, 12, 405–406.
3. According to IUPAC, “oxidation state of an atom is the charge of this atom after ionic approximation of its heteronuclear bonds.” IUPAC Compendium of Chemical Terminology. 10.1351/goldbook.O04365. See also Refs. 18 - 20 .
4. Harder S; Piers WE Organometallic and coordination chemistry of the s-block metals. Dalton Trans. 2018, 47, 12491–12492. [PubMed: 30191944]
5. Krieck S; Westerhausen M Kudos and Renaissance of s-Block Metal Chemistry. Inorganics 2017, 5, 17.
6. Hill MS; Liptrot DJ; Weetman C Alkaline earths as main group reagents in molecular catalysis. Chem. Soc. Rev 2016, 45, 972–988. [PubMed: 26797470]
7. Evans WJ The Importance of Questioning Scientific Assumptions: Some Lessons from f Element Chemistry. Inorg. Chem 2007, 46, 3435–3449. [PubMed: 17428046]
8. Arnold PL; McMullon MW; Rieb J; Kühn FE C—H Bond Activation by f-Block Complexes. Angew. Chem. Int. Ed 2015, 54, 82–100.
9. Astruc D Electron Transfer and Radical Processes in Transition Metal Chemistry; Wiley-VCH: New York, 1995.
10. Labinger JA Tutorial on Oxidative Addition. Organometallics 2015, 34, 4784–4795.

11. Kočovský P; Malkov AV; Vyskočil Š; Lloyd-Jones GC Transition metal catalysis in organic synthesis: reflections, chirality and new vistas. Pure Appl. Chem 1999, 71, 1425–1433.
12. King AO; Yasuda N Palladium-Catalyzed Cross-Coupling Reactions in the Synthesis of Pharmaceuticals. In Organometallics in Process Chemistry; Larsen RD, Ed.; Springer: Berlin, Heidelberg, 2004; pp 205–245.
13. Corbet J-P; Mignani G Selected Patented Cross-Coupling Reaction Technologies. Chem. Rev 2006, 106, 2651–2710. [PubMed: 16836296]
14. Johansson Seechurn CCC; Kitching MO; Colacot TJ; Snieckus V Palladium-Catalyzed Cross-Coupling: A Historical Contextual Perspective to the 2010 Nobel Prize. Angew. Chem. Int. Ed 2012, 51, 5062–5085.
15. Girolami G Origin of the Terms *Pnictogen* and *Pnictide*. J. Chem. Educ 2009, 86, 1200–1201.
16. Fluck E New Notations in the Periodic Table. Pure Appl. Chem 1988, 60, 431–436.
17. In line with the view articulated by Vitz (Ref. 18) and endorsed by Karen et al. (Ref. 19), we consider for the purpose of this Perspective that redox (oxidation/reduction) reactions are "…those in which oxidation states of the reactant(s) change." Organopnictogen redox catalysis therefore concerns catalytic transformations operating by a closed cycle of elementary reactions involving oxidation state changes at the catalytic pnictogen center.
18. Vitz E Redox Redux: Recommendations for Improving Textbook and IUPAC Definitions. J. Chem. Educ 2002, 79, 397–400.
19. Karen P; McArdle P; Takats J Comprehensive definition of oxidation state (IUPAC Recommendations 2016). Pure Appl. Chem 2016, 88, 831–839.
20. Karen P Oxidation State, A Long-Standing Issue! Angew. Chem. Int. Ed 2015, 54, 4716–4726.
21. For an insightful discourse on the oxidation state formalism and its connection to related descriptors, see: Parkin G Valence, Oxidation Number, and Formal Charge: Three Related but Fundamentally Different Concepts. J. Chem. Educ 2006, 83, 791–799.
22. As correctly noted by a reviewer and reinforced by the IUPAC recommendations, 'oxidation state' is a formalism, and "[i]t is therefore not surprising that, for some compounds, one value does not fit all uses, or that dedicated measurements or computations are needed to ascertain the actual [oxidation state]" (Ref. 19). Especially in main group chemistry, questions about the assignment of nominal oxidation states have given rise to much critical (and colorful) analysis, as in Refs. 23-25.
23. Himmel D; Krossing I; Schnepf A Dative Bonds in Main-Group Compounds: A Case for Fewer Arrows! Angew. Chem. Int. Ed 2014, 53, 370–374.
24. Frenking G Dative Bonds in Main-Group Compounds: A Case for More Arrows! Angew. Chem. Int. Ed 2014, 53, 6040–6046.
25. Himmel D; Krossing I; Schnepf A Dative or Not Dative? Angew. Chem. Int. Ed 2014, 53, 6047–6048.
26. Davy H XIV. Researches on the oxymuriatic acid, its nature and combinations; and on the elements of the muriatic acid. With some experiments on sulphur and phosphorus, made in the laboratory of the Royal Institution. Phil. Trans. Royal Soc 1810, 100, 231–267.
27. Davy H XXII. On some combinations of phosphorus and sulphur, and on some other subjects of chemical inquiry. Phil. Trans. Royal Soc 1812, 102, 405–415.
28. Staudinger H; Meyer J Über neue organische Phosphorverbindungen III. Phosphinmethylenderivate und Phosphinimine. Helv. Chim. Acta 1919, 2, 635–646.
29. Gololobov YG; Zhmurova IN; Kasukhin LF Sixty Years of Staudinger Reaction. Tetrahedron 1981, 37, 437–472.
30. Gololobov YG; Kasukhin LF Recent Advances in the Staudinger Reaction. Tetrahedron 1992, 48, 1353–1406.
31. Núñez MG; Farley AJM; Dixon DJ Bifunctional Iminophosphorane Organocatalysts for Enantioselective Synthesis: Application to the Ketimine Nitro-Mannich Reaction. J. Am. Chem. Soc 2013, 135, 16348–16351. [PubMed: 24107070]
32. Krawczyk H; Dzięgielewski M; Deredas D; Albrecht A; Albrecht Ł Chiral Iminophosphoranes—An Emerging Class of Superbase Organocatalysts. Chem. Eur. J 2015, 21, 10268–10277. [PubMed: 25924847]

33. Formica M; Rozsar D; Su G; Farley AJM; Dixon DJ Bifunctional Iminophosphorane Superbase Catalysis: Applications in Organic Synthesis. Acc. Chem. Res 2020, 53, 2235–2247. [PubMed: 32886474]
34. Saxon E; Bertozzi CR Cell Surface Engineering by a Modified Staudinger Reaction. Science 2000, 287, 2007–2010. [PubMed: 10720325]
35. Köhn M; Breinbauer R The Staudinger Ligation–A Gift to Chemical Biology. Angew. Chem. Int. Ed 2004, 43, 3106–3116.
36. van Berkel SS; van Eldijk MB; van Hest JCM Staudinger Ligation as a Method for Bioconjugation. Angew. Chem. Int. Ed 2011, 50, 8806–8827.
37. Schilling CI; Jung N; Biskup M; Schepers U; Bräse S Bioconjugation *via* azide-Staudinger ligation: an overview. Chem. Soc. Rev 2011, 40, 4840–4871. [PubMed: 21687844]
38. Liu S; Edgar KJ Staudinger Reactions for Selective Functionalization of Polysaccharides: A Review. Biomacromolecules 2015, 16, 2556–2571. [PubMed: 26245299]
39. Bednarek C; Wehl I; Jung N; Schepers U; Bräse S The Staudinger Ligation. Chem. Rev 2020, 120, 4301–4354. [PubMed: 32356973]
40. Wittig G; Schöllkopf U Über Triphenyl-phosphin-methylene als olefinbildende Reagenzien (I. Mitteil.). Chem. Ber 1954, 87, 1318–1330.
41. Wittig G; Haag W Über Triphenyl-phosphin-methylene als olefinbildende Reagenzien (II. Mitteil.). Chem. Ber 1955, 88, 1654–1666.
42. Hoffmann RW Wittig and His Accomplishments: Still Relevant Beyond His 100th Birthday. Angew. Chem. Int. Ed 2001, 40, 1411–1416.
43. Pommer H The Wittig Reaction in Industrial Practice. Angew. Chem. Int. Ed 1977, 16, 423–492.
44. Barton DHR; Charpiot B; Motherwell WB Regiospecific Arylation by Acid/Base Controlled Reactions of Tetraphenylbismuth Ester. Tetrahedron Lett. 1982, 23, 3365–3368.
45. Barton DHR; Bhatnagar NY; Blazejewski J-C; Charpiot B; Finet J-P; Lester DJ; Motherwell WB; Papoula MTB; Stanforth SP Pentavalent Organobismuth Reagents. Part 2. The Phenylation of Phenols. J. Chem. Soc., Perkin Trans. 1 1985, 2657–2665.
46. Barton DHR; Blazejewski J-C; Charpiot B; Finet J-P; Motherwell WB; Papoula MTB; Stanforth SP Pentavalent Organobismuth Reagents. Part 3. Phenylation of Enols and of Enolate and other Anions. J. Chem. Soc., Perkin Trans. 1 1985, 53, 2667–2675.
47. Dagorne S; Wehmschulte R Recent Developments on the Use of Group 13 Metal Complexes in Catalysis. ChemCatChem 2018, 10, 2509–2520.
48. Von Grotthuss E; Prey SE; Bolte M; Lerner HW; Wagner M Dual Role of Doubly Reduced Arylboranes as Dihydrogen- and Hydride-Transfer Catalysts. J. Am. Chem. Soc 2019, 141, 6082–6091. [PubMed: 30875474]
49. Légaré MA; Pranckevicius C; Braunschweig H Metallomimetic Chemistry of Boron. Chem. Rev 2019, 119, 8231–8261 [PubMed: 30640447]
50. Su Y; Kinjo R Small Molecule Activation by Boron-Containing Heterocycles. Chem. Soc. Rev 2019, 48, 3613–3659. [PubMed: 30977491]
51. Revunova K; Nikonov GI Main Group Catalysed Reduction of Unsaturated Bonds. Dalt. Trans 2014, 44, 840–866.
52. Hadlington TJ; Driess M; Jones C Low-Valent Group 14 Element Hydride Chemistry: Towards Catalysis. Chem. Soc. Rev 2018, 47, 4176–4197. [PubMed: 29666847]
53. Freudendahl DM; Santoro S; Shahzad SA; Santi C; Wirth T Green Chemistry with Selenium Reagents: Development of Efficient Catalytic Reactions. Angew. Chem. Int. Ed 2009, 48, 8409–8411.
54. Breder A; Ortgies S Recent Developments in Sulfur- and Selenium-Catalyzed Oxidative and Isohypsic Functionalization Reactions of Alkenes. Tetrahedron Lett. 2015, 56, 2843–2852.
55. Ortgies S; Breder A Oxidative Alkene Functionalizations via Selenium-**π**-Acid Catalysis. ACS Catal. 2017, 7, 5828–5840.
56. Shao L; Li Y; Lu J; Jiang X Recent Progress in Selenium-Catalyzed Organic Reactions. Org. Chem. Front 2019, 6, 2999–3041.
57. Singh FV; Wirth T Selenium Reagents as Catalysts. Catal. Sci. Technol 2019, 9, 1073–1091.

58. Matviitsuk A; Panger JL; Denmark SE Catalytic, Enantioselective Sulfenofunctionalization of Alkenes: Development and Recent Advances. Angew. Chem. Int. Ed 2020, 59, 19796–19819.
59. Stang PJ; Zhdankin VV Organic Polyvalent Iodine Compounds. Chem. Rev 1996, 96, 1123–1173. [PubMed: 11848783]
60. Dohi T; Maruyama A; Yoshimura M; Morimoto K; Tohma H; Kita Y Versatile Hypervalent-Iodine(III)-Catalyzed Oxidations with m-Chloroperbenzoic Acid as a Cooxidant. Angew. Chem. Int. Ed 2005, 44, 6193–6196.
61. Richardson RD; Wirth T Hypervalent Iodine Goes Catalytic. Angew. Chem. Int. Ed 2006, 45, 4402–4404.
62. Dohi T; Kita Y Hypervalent iodine reagents as a new entrance to organocatalysts. Chem. Commun 2009, 2073–2085.
63. Singh FV; Wirth T Hypervalent Iodine-Catalyzed Oxidative Functionalizations Including Stereoselective Reactions. Chem. Asian J 2014, 9, 950–971. [PubMed: 24523252]
64. Arnold AM; Ulmer A; Gulder T Advances in Iodine(III)-Mediated Halogenations: A Versatile Tool to Explore New Reactivities and Selectivities. Chem. Eur. J 2016, 22, 8728–8739. [PubMed: 27061937]
65. Yoshimura A; Zhdankin VV Advances in Synthetic Applications of Hypervalent Iodine Compounds. Chem. Rev 2016, 116, 3328–3435. [PubMed: 26861673]
66. Li X; Chen P; Liu G Recent advances in hypervalent iodine(III)-catalyzed functionalization of alkenes. Beilstein J. Org. Chem 2018, 14, 1813–1825. [PubMed: 30112085]
67. Flores A; Cots E; Berges J; Muniz K Enantioselective Iodine(I/III) Catalysis in Organic Synthesis. Adv. Synth. Catal 2019, 361, 2–25.
68. Lee H; Choi S; Hong K Difunctionalization Using Hypervalent Iodine Reagents: Progress and Developments in the Past Ten Years. Molecules 2019, 24, 2634.
69. Power PP Main-group elements as transition metals. Nature 2010, 463, 171–177. [PubMed: 20075912]
70. Chu T; Nikonov GI Oxidative Addition and Reductive Elimination at Main-Group Element Centers. Chem. Rev 2018, 118, 3608–3680. [PubMed: 29558125]
71. Weetman S; Inoue S The Road Travelled: After Main-Group Elements as Transiton Metals. ChemCatChem 2018, 10, 4213–4228.
72. Melen R Frontiers in molecular p-block chemistry: From structure to reactivity. Science 2019, 363, 479–484. [PubMed: 30705183]
73. Ruffell K; Ball LT Organobismuth Redox Manifolds: Versatile Tools for Synthesis. Trends Chem. 2020, 2, 867–869.
74. Abbenseth J; Goicoechea JM Recent developments in the chemistry of non-trigonal pnictogen pincer compounds: from bonding to catalysis. Chem. Sci 2020, 11, 9728–9740.
75. Hu Z; Gao S Upper crustal abundance of trace elements: A revision and update. Chem. Geol 2008, 253, 205–221.
76. U.S. Geological Survey Mineral Commodity Summaries 2020, Reston, VA, 2020, 10.3133/mcs2020.
77. Caputo CB; Hounjet LJ; Dobrovetsky R; Stephan DW Lewis Acidity of Organofluorophosphonium Salts: Hydrodefluorination by a Saturated Acceptor. Science 2013, 341, 1374–1377. [PubMed: 24052304]
78. Bayne JM; Stephan DW Phosphorus Lewis acids: emerging reactivity and applications in catalysis. Chem. Soc. Rev 2016, 45, 765–774. [PubMed: 26255595]
79. Werner T Phosphonium Salt Organocatalysis. Adv. Synth. Catal 2009, 351, 1469–1481.
80. Denmark SE; Beutner GL Lewis Base Catalysis in Organic Synthesis. Angew. Chem. Int. Ed 2008, 47, 1560–1638.
81. Wei Y; Shi M Applications of Chiral Phosphine-Based Organocatalysts in Catalytic Asymmetric Reactions. Chem. Asian J 2014, 9, 2720–2734. [PubMed: 24819715]
82. Guo H; Fan YC; Sun Z; Wu Y; Kwon O Phosphine Organocatalysis. Chem. Rev 2018, 118, 10049–10293. [PubMed: 30260217]

83. Stephan DW “Frustrated Lewis pairs”: a concept for new reactivity and catalysis. Org. Biomol. Chem 2008, 6, 1535–1539. [PubMed: 18421382]
84. Stephan DW Frustrated Lewis pairs: a new strategy to small molecule activation and hydrogenation catalysis. Dalton Trans. 2009, 3129–3136. [PubMed: 19421613]
85. Stephan DW; Erker G Frustrated Lewis Pairs: Metal-free Hydrogen Activation and More. Angew. Chem. Int. Ed 2010, 49, 49–76.
86. Stephan DW Frustrated Lewis Pairs: From Concept to Catalysis. Acc. Chem. Res 2015, 48, 306–316. [PubMed: 25535796]
87. Transition Metal Complexes of Phosphorus, Arsenic and Antimony Ligands; McAuliffe CA, Ed. MacMillan: London, 1973.
88. Tolman CA Steric Effects of Phosphorus Ligands in Organometallic Chemistry and Homogeneous Catalysis. Chem. Rev 1977, 77, 313–348.
89. Champness NR; Levason R Coordination chemistry of stibine and bismuthine ligands. Coord. Chem. Rev 1994, 133, 115–217.
90. Burt J; Levason W; Reid G Coordination chemistry of the main group elements with phosphine, arsine, and stibine ligands. Coord. Chem. Rev 2004, 260, 65–115.
91. Levason W; Reid G Development in the coordination chemistry of stibine ligands. Coord. Chem. Rev 2006, 250, 2565–2594.
92. Martin R; Buchwald SB Palladium-Catalyzed Suzuki–Miyaura Cross-Coupling Reactions Employing Dialkylbiaryl Phosphine Ligands. Acc. Chem. Res 2008, 41, 1461–1473. [PubMed: 18620434]
93. Phosphorus Ligands in Asymmetric Catalysis: Synthesis and Applications; Börner A, Ed. Wiley-VCH: Weinheim, 2008.
94. Jones JS; Gabbaï FP Coordination- and Redox-Noninnocent Behavior of Ambiphilic Ligands Containing Antimony. Acc. Chem. Res 2016, 49, 857–867. [PubMed: 27092722]
95. Greenwood NN; Earnshaw A Chemistry of the Elements, 2nd ed.; Elsevier Butterworth-Heinemann: Oxford, UK, 1997.
96. Burford N; Carpenter Y-Y; Conrad E; Saunders CDL The Chemistry of Arsenic, Antimony, and Bismuth. In Biological Chemistry of Arsenic, Antimony and Bismuth; Sun H, Ed.; Wiley: Hoboken, NJ, 2010; pp 1–17.
97. Zhao L; Pan S; Holzmann N; Schwerdtfeger P; Frenking G Chemical Bonding and Bonding Models of Main-Group Compounds. Chem. Rev 2019, 119, 8781–8845. [PubMed: 31251603]
98. Power PP π-Bonding and the Lone Pair Effect in Multiple Bonds Involving Heavier Main Group Elements. Chem. Rev 1999, 99, 3463–3503. [PubMed: 11849028]
99. Fischer RC; Power PP π-Bonding and the Lone Pair Effect in Multiple Bonds Involving Heavier Main Group Elements: Developments in the New Millennium. Chem. Rev 2010, 110, 3877–3923. [PubMed: 20672858]
100. Power PP An Update on Multiple Bonding between Heavier Main Group Elements: The Importance of Pauli Repulsion, Charge-Shift Character, and London Dispersion Force Effect. Organometallics 2020, 39, 4127–4138.
101. Desclaux J Relativistic Dirac-Fock expectation values for atoms with Z= 1 to Z= 120. At. Data Nucl. Data Tables 1973, 12, 311–406.
102. Pyykkö P Interpretation of secondary periodicity in the periodic system. J. Chem. Res. Synop 1979, 380–381.
103. Imyanitov NS Does the period table appear doubled? Two variants of division of elements into two subsets. Internal and secondary periodicity. Found. Chem 2019, 21, 255–284.
104. Seth M; Dolg M; Fulde P; Schwerdtfeger P Lanthanide and Actinide Contractions: Relativistic and Shell Structure Effects. J. Am. Chem. Soc 1995, 117, 6597–6598.
105. Wang Z-L; Hu H-S; von Sventály L; Stoll H; Fritzsche S; Pyykkö P; Schwarz WHE; Li J Understanding the Uniqueness of 2p Elements in Periodic Tables. Chem. Eur. J 2020, 26, 15558–15564. [PubMed: 32975862]

106. Pyykkö P Dirac–Fock One-centre Calculaions. Part 7.–Divalent Systems MH+ and MH2 (M = Be, Mg, Ca, Sr, Ba, Ra, Zn, Cd, Hg, Yb and No). J. Chem. Soc., Faraday Trans. 2 1979, 75, 1256–1276.
107. Pyykkö P Dirac-Fock One-centre Calculations Part 8. The $^{1}\Sigma$ states of ScH, YH, LaH, AcH, TmH, LuH and LrH. Physica Scripta 1979, 20, 647–651.
108. Kaupp M The Role of Radial Nodes of Atomic Orbitals for Chemical Bonding and the Periodic Table. J. Comput. Chem 2007, 28, 320–325. [PubMed: 17143872]
109. Kaupp M Chemical Bonding of Main-Group Elements. The Chemical Bond. 2014, 1, 1–24.
110. Desclaux JP; Kim Y-K Relativistic effects in outer shells of heavy atoms. J. Phys. B 1975, 8, 1177–1182.
111. Pitzer K Relativistic Effects on Chemical Properties. Acc. Chem. Res 1979, 12, 271–276.
112. Pyykkö P; Desclaux J-P Relativity and the Periodic System of Elements. Acc. Chem. Res 1979, 12, 276–281.
113. Pyykkö P Relativistic Effects in Structural Chemistry. Chem. Rev 1988, 88, 563–594.
114. Bagus PS; Lee YS; Pitzer KS Effects of Relativity and of the Lanthanide Contraction on the Atoms from Hafnium to Bismuth. Chem. Phys. Lett 1975, 33, 408–411.
115. Kutzelnigg W Chemical Bonding in Higher Main Group Elements. Angew. Chem. Int. Ed 1984, 23, 272–295.
116. Kutzelnigg W Orthogonal and Non-orthogonal Hybrids. J. Mol. Struct 1988, 169, 403–419.
117. Balasubramanian K; Chung YS; Glaunsinger WS Geometries and bond energies of PH_n and PH_n^+ (n=1–3). J. Chem. Phys 1993, 98, 8859–8869.
118. Dai D; Balasubramanian K Geometries and energies of electronic states of AsH*3*, SbH*3*, and BiH*3* and their positive ions. J. Chem. Phys 1990, 93, 1837–1846.
119. Groom CR; Bruno IJ; Lightfoot MP; Ward SC The Cambridge Structural Database. Acta Cryst. B 2016, 72, 171–179.
120. Dunne BJ; Orpen AG Triphenylphosphine: a Redetermination. Acta Cryst. C 1991, 47, 345–347.
121. Sobolev AN; Belsky VK; Chernikova NY; Akhmadulina FY Structure Analysis of Triaryl Derivatives of the Group V Elements: VIII. The Crystal and Molecular Structure of Triphenylarsine, C18H15As. J. Organomet. Chem 1983, 244, 129–136.
122. Adams EA; Kolis JW; Pennington WT Structure of Triphenylstibine. Acta Cryst. C 1990, 46, 917–919.
123. Bučinský L; Jayatilaka D; Grabowsky S Importance of Relativistic Effects and Electron Correlation in Structure Factors and Electron Density of Diphenyl Mercury and Triphenyl Bismuth. J. Phys. Chem. A 2016, 120, 6650–6669. [PubMed: 27434184]
124. Schwerdtfeger P; Laakonen L; Pyykkö P Trends in inversion barriers. I. Group-15 hydrides. J. Chem. Phys 1992, 96, 6807–6819.
125. Schwerdtfeger P; Boyd PDW; Fischer T; Hunt P; Liddell M Trends in Inversion Barriers of Group 15 Compounds. 2. Ab-Initio and Density Functional Calculations on Group 15 Fluorides. J. Am. Chem. Soc 1994, 116, 9620–9633.
126. Santiago RT; Haiduke RLA Relativistic effects on inversion barriers of pyramidal group 15 hydrides. Int. J. Quantum Chem 2018, 118, e25585.
127. Levin C A Qualitative Molecular Orbital Picture of Electronegativity Effects on XH_3 Inversion Barriers. J. Am. Chem. Soc 1975, 97, 5649–5655.
128. Lee K; Blake AV; Tanushi A; McCarthy SM; Kim D; Loria SM; Donahue CM; Spielvogel KD; Keith JM; Daly SR; Radosevich AT Validating the Biphilic Hypothesis of Nontrigonal Phosphorus(III) Compounds. Angew. Chem. Int. Ed 2019, 58, 6993–6998.
129. Kindervater MB; Marczenko KM; Werner-Zwanziger U; Chitnis SS A Redox-Confused Bismuth(I/III) Triamide with a T-Shaped Planar Ground State. Angew. Chem. Int. Ed 2019, 58, 7850–7855.
130. Marczenko KM; Zurakowski JA; Kindervater MB; Jee S; Hynes T; Roberts N; Park S; Werner-Zwanziger U; Lumsden M; Langelaan DN; Chitnis SS Periodicity in Structure, Bonding, and Reactivity for p-Block Complexes of a Geometry Constraining Triamide Ligand. Chem. Eur. J 2019, 25, 16414–16424. [PubMed: 31574185]

131. Marczenko KM; Jee S; Chitnis SS High Lewis Acidity at Planar, Trivalent, and Neutral Bismuth Centers. Organometallics 2020, 39, 4287–4296.

132. Wittig G; Rieber M Darstellung und Eigenschaften des Pentaphenyl-phosphors. Justus Liebiegs Ann. Chem 1949, 562, 187–192.

133. Wittig G; Clauß K Pentaphenyl-arsen und Pentaphenyl-antimon. Justus Liebigs Ann. Chem 1952, 577, 26–39.

134. Wittig G; Clauß K Pentaphenyl-wismut. Justus Liebegs Ann. Chem 1952, 578, 136–146.

135. Wheatley PJ 408. The Crystal and Molecular Structure of Pentaphenyl-phosphorus. J. Chem. Soc 1964, 2206–2222.

136. Brock CP; Webster DF The Crystal structure of Pentaphenylarsenic: Implications for the Role of Crystal Packing Forces in the Structures of Penta-aryl Group V Molecules. Acta. Cryst. B 1976, 32, 2089–2094.

137. Beauchamp AL; Bennett MJ; Cotton FA A Reinvestigation of the Crystal and Molecular Structure of Pentaphenylantimony. J. Am. Chem. Soc 1968, 90, 6675–6680.

138. Schmuck A; Buschmann J; Fuchs J; Seppelt K Structure and Color of Pentaphenylbismuth. Angew. Chem. Int. Ed 1987, 26, 1180–1182.

139. Addison AW; Rao TN; Reedijk J; van Rijn J; Verschoor GC Synthesis, structure, and spectroscopic properties of copper(II) compounds containing nitrogen–sulphur donor ligands; the crystal and molecular structure of aqua[1,7-bis(N-methylbenzimidazol-2′-yl)-2,6-dithiaheptane]copper(II) perchlorate. J.Chem. Soc., Dalton Trans 1984, 1349–1356.

140. The structural parameter τ is defined for 5-coordiante compounds as $\tau = (\beta - \alpha)/60^{o}$, where $\beta > \alpha$ are the two largest valence angles of the coordination center. At the two extremes, $\tau = 0$ for ideal square pyramidal and $\tau = 1$ for ideal trigonal bipyramidal geometries.

141. Ugi I; Marquarding D; Klusacek H; Gillespie P; Ramirez F Berry Pseudorotation and Turnstile Rotation. Acc. Chem. Res 1971, 4, 288–296.

142. Gillespie P; Hoffman P; Klusacek H; Marquarding D; Pfohl S; Ramirez F; Tsolis EA; Ugi I Non-rigid Molecular Skeletons—Berry Pseudorotation and Turnstile Rotation. Angew. Chem. Int. Ed 1971, 10, 687–715.

143. Beattie IR; Livingston KMS; Ozin GA; Sabine R The Shape of Pentaphenylantimony and Pentaphenylarsenic in Solution. J. Chem. Soc., Dalton Trans 1972, 784–786.

144. Schmuck A; Seppelt K Strukturen von Pentaarylbismut-Verbindungen. Chem. Ber 1989, 122, 803–808.

145. Schmuck A; Leopold D; Wallenhauer S; Seppelt K Strukturen von Pentaarylbismut-Verbindungen. Chem. Ber 1990, 123, 761–766.

146. Schmuck A; Seppelt K; Pyykkö P Structure and Color of Substituted Pentaphenylbismuth. Angew. Chem. Int. Ed 1990, 29, 213–215.

147. Seppelt K Structure, Color, and Chemistry of Pentaaryl Bismuth Compounds. Adv. Organomet. Chem 1992, 34, 207–217.

148. Barton DHR; Blazejewski J-C; Charpiot B; Lester DJ; Motherwell WG; Papoula MTB Comparative Arylation Reactions with Pentaphenylbismuth and with Triphenylbismuth Carbonate. J. Chem. Soc., Chem. Commun 1980, 827–829.

149. Kuczkowski A; Schulz S; Nieger M; Schreiner PR Experimental and Computational Studies of $R_3Al\text{-}ER'_3$ (E = P, As, Sb, Bi; R = Et, *t*-Bu; R′ = $SiMe_3$, *i*-Pr) Donor–Acceptor Complexes: Role of the Central Pnictine and the Substituents on the Structure and Stability of Alane Adducts. Organometallics 2002, 21, 1408–1419.

150. Henry MC; Wittig G The Organometallic Alkylidene Reaction. J. Am. Chem. Soc 1960, 82, 563–564.

151. Matano Y Synthesis, Structure, and Reactions of Triaryl(methyl)bismuthonium Salts. Organometallics 2000, 19, 2258–2263.

152. Tolman CA Phosphorus Ligand Exchange Equilibriums on Zerovalent Nickel. Dominant Role for Steric Effects. J. Am. Chem. Soc 1970, 92, 2956–2965.

153. Tolman CA Steric Effects of Phosphorus Ligands in Organometallic Chemistry and Homogeneous Catalysis. Chem. Rev 1977, 77, 313–348.

154. Levason W; McAuliffe CA Coordination Chemistry of Organostibines. Acc. Chem. Res 1978, 11, 363–368.

155. Nitrogen, Phosphorus, Arsenic, Antimony, and Bismuth. In Standard Potentials in Aqueous Solution; Bard AJ, Parsons R, Jordan J, Eds.; CRC Press: Boca Raton, FL, 1985; pp 127–187.

156. For Group 15 Frost diagrams similar to Figure 6, see Refs. 95 and 96.

157. Drago RS Thermodynamic Evaluation of the Inert Pair Effect. J. Phys. Chem 1958, 62, 353–357.

158. Sanderson RT The “Inert-Pair Effect” on Electronegativity. Inorg. Chem 1986, 25, 1856–1858.

159. Wheeler RA; Kumar PNVP Stereochemically Active or Inactive Lone Pair Electrons in Some Six-Coordinate, Group 15 Halides. J. Am. Chem. Soc 1992, 114, 4776–4784.

160. Naito T; Nagase S; Yamataka H Theoretical Study of the Structure and Reactivity of Ylides of N, P, As, Sb, and Bi. J. Am. Chem. Soc 1994, 116, 10080–10088.

161. Fischer J; Rudzitis E Preparation, Properties and Reactions of Bismuth Pentafluoride. J. Am. Chem. Soc 1959, 81, 6375–6377.

162. Gerstenberger MRC; Haas A Methods of Fluorination in Organic Chemistry. Angew. Chem. Int. Ed 1981, 20, 647–667.

163. Breidung J; Thiel W A Systematic *Ab Initio* Study of the Group V Trihalides MX_3 and Pentahalides MX_5 (M = P–Bi, X = F–I). J. Comput. Chem 1992, 13, 165–176.

164. Schwerdtfeger P; Heath GA; Dolg M; Bennett MA Low Valencies and Periodic Trends in Heavy Element Chemistry. A Theoretical Study of Relativistic Effects and Electron Correlation Effects in Group 13 and Period 6 Hydrides and Halides. J. Am. Chem. Soc 1992, 114, 7518–7527.

165. Moc J; Morokuma K Ab Initio Molecular Orbital Study on the Periodic Trends in Structures and Energies of Hypervalent Compounds: Five-Coordinated XH_5 Species Containing a Group 15 Central Atom (X = P, As, Sb, and Bi). J. Am. Chem. Soc 1995, 117, 11790–11797.

166. Barton DHR; Motherwell WB; Stobie A A Catalytic Method for α-Glycol Cleavage. J. Chem. Soc., Chem. Commun 1981, 1232–1233.

167. Cahours A; Hofmann AW Untersuchungen Über Die Phosphorbasen. Ann. der Chemie und Pharm 1857, 104, 1–39.

168. Wiley GA; Hershkowitz RL; Rein BM; Chung BC Studies in Organophosphorus Chemistry. I. Conversion of Alcohols and Phenols to Halides by Tertiary Phosphine Dihalides. J. Am. Chem. Soc 1964, 86, 964–965.

169. Cadogan JIG; Mackie RK Tervalent Phosphorus Compounds in Organic Synthesis. Chem. Soc. Rev 1974, 3, 87–137.

170. Denney DB; DiLeone RR Reactions of T-Alkyl Hypochlorites with Trisubstituted Phosphines and Phosphites. J. Am. Chem. Soc 1962, 84, 4737–4743

171. Rabinowitz R; Marcus R Ylid Intermediate in the Reaction of Triphenylphosphine with Carbon Tetrachloride. J. Am. Chem. Soc 1962, 84, 1312–1313.

172. Lee JB Preparation of Acyl Halides under Very Mild Conditions. J. Am. Chem. Soc 1966, 88, 3440–3441.

173. Mukaiyama T; Ueki M; Maruyama H; Matsueda R A New Method for Peptide Synthesis by Oxidation-Reduction Condensation. J. Am. Chem. Soc 1968, 90, 4490–4491. [PubMed: 5666352]

174. Denney DB; Jones DH The Peroxide Route to Pentaoxyphosphoranes. J. Am. Chem. Soc 1969, 91, 5821–5825.

175. Appel R Tertiary Phosphane/Tetrachloromethane, a Versatile Reagent for Chlorination, Dehydration, and P–N Linkage. Angew. Chem. Int. Ed 1975, 14, 801–811.

176. Bartlett PD; Baumstark AL; Landis ME Insertion Reaction of Triphenylphosphine with Tetramethyl-1,2-Dioxetane. Deoxygenation of a Dioxetane to an Epoxide. J. Am. Chem. Soc 1973, 95, 6486–6487.

177. Skowrońska A; Pakulski M; Michalski J; Cooper D; Trippett S The Arbuzov Reaction of Triethyl Phosphite with Elemental Iodine. Tetrahedron Lett. 1980, 21, 321–322.

178. Krenske EH Reductions of Phosphine Oxides and Sulfides by Perchlorosilanes: Evidence for the Involvement of Donor-Stabilized Dichlorosilylene. J. Org. Chem 2012, 77, 1–4. [PubMed: 22148631]

179. Covitz F; Westheimer FH The Hydrolysis of Methyl Ethylene Phosphate: Steric Hindrance in General Base Catalysis. J. Am. Chem. Soc 1963, 85, 1773–1777.

180. Naumann K; Zon G; Mislow K The Use of Hexachlorodisilane as a Reducing Agent. Stereospecific Deoxygenation of Acyclic Phosphine Oxides. J. Am. Chem. Soc 1969, 91, 7012–7023.

181. Imamoto T; Kikuchi SI; Miura T; Wada Y Stereospecific Reduction of Phosphine Oxides to Phosphines by the Use of a Methylation Reagent and Lithium Aluminum Hydride. Org. Lett 2001, 3, 87–90. [PubMed: 11429879]

182. Keglevich G; Gaumont AC; Denis JM Selective Reductions in the Sphere of Organophosphorus Compounds. Heteroat. Chem 2001, 12, 161–167.

183. Bryan MC; Dunn PJ; Entwistle D; Gallou F; Koenig SG; Hayler JD; Hickey MR; Hughes S; Kopach ME; Moine G; Richardson P; Roschangar F; Steven A; Weiberth FJ Key Green Chemistry research areas from a pharmaceutical manufacturers' perspective revisited. Green Chem. 2018, 20, 5082–5103.

184. Krenske EH Theoretical Investigation of the Mechanisms and Stereoselectivities of Reductions of Acyclic Phosphine Oxides and Sulfides by Chlorosilanes. J. Org. Chem 2012, 77, 3969–3977. [PubMed: 22497492]

185. van Kalkeren HA; Leenders SHAM; Hommersom CRA; Rutjes FPJT; van Delft FL In Situ Phosphine Oxide Reduction: A Catalytic Appel Reaction. Chem. Eur. J 2011, 17, 11290–11295. [PubMed: 21882274]

186. Keglevich G; Fekete M; Chuluunbaatar T; Dobó A; Harmat V; Toke L One-pot transformation of cyclic phosphine oxides to phosphine–boranes by dimethyl sulfide–borane. J. Chem. Soc., Perkin Trans. 1 2000, 4451–4455.

187. Hérault D; Nguyen DH; Nuel D; Buono G Reduction of secondary and tertiary phosphine oxides to phosphines. Chem. Soc. Rev 2015, 44, 2508–2528. [PubMed: 25714261]

188. Mann FG; Watson J Conditions of Salt Formation in Polyamines and Kindred Compounds. Salt Formation in the Tertiary 2-Pyridylamines, Phosphines and Arsines. J. Org. Chem 1948, 13, 502–531.

189. Newkome GR; Hager DC A New Contractive Coupling Procedure. Convenient Phosphorus Expulsion Reaction. J. Am. Chem. Soc 1978, 100, 5567–5568.

190. Uchida Y; Kozawa H Formation of 2,2′-Bipyridyl by Ligand Coupling on the Phosphorus Atom. Tetrahedron Lett. 1989, 30, 6365–6368.

191. Uchida Y; Onoue K; Tada N; Nagao F; Oae S Ligand Coupling Reaction on the Phosphorus Atom. Tetrahedron Lett. 1989, 30, 567–570.

192. Uchida Y; Kawai M; Masauji H; Oae S Reactions of Triarylphosphines with Organolithium Reagents. Formation of Biaryls. Heteroat. Chem 1993, 4, 421–426.

193. Hilton MC; Zhang X; Boyle BT; Alegre-Requena JV; Paton RS; McNally A Heterobiaryl Synthesis by Contractive C–C Coupling via P(V) Intermediates. Science 2018, 362, 799–804. [PubMed: 30442804]

194. Koniarczyk JL; Greenwood JW; Alegre-Requena JV; Paton RS; McNally A A Pyridine–Pyridine Cross-Coupling Reaction via Dearomatized Radical Intermediates. Angew. Chem. Int. Ed 2019, 58, 14882–14886.

195. Boyle BT; Hilton MC; McNally A Nonsymmetrical Bis-Azine Biaryls from Chloroazines: A Strategy Using Phosphorus Ligand-Coupling. J. Am. Chem. Soc 2019, 141, 15441–15449. [PubMed: 31483634]

196. van Kalkeren HA; van Delft FL; Rutjes FPJT Organophosphorus Catalysis to Bypass Phosphine Oxide Waste. ChemSusChem 2013, 6, 1615–1624. [PubMed: 24039197]

197. Marsden SP Catalytic Variants of Phosphine Oxide-Mediated Organic Transformations. In Sustainable Catalysis; Dunn PJ, Hii KK, Krische MJ, Williams MT, Eds.; Wiley: New York, 2013; pp 339–361.

198. Voituriez A; Saleh N From phosphine-promoted to phosphine-catalyzed reactions by in situ phosphine oxide reduction. Tetrahedron Lett. 2016, 57, 4443–4451.

199. Longwitz L; Werner T Recent advances in catalytic Wittig-type reactions based on P(III)/P(V) redox cycling. Pure Appl. Chem 2019, 91, 95–102.

200. O'Brien CJ; Tellez JL; Nixon ZS; Kang LJ; Carter AL; Kunkel SR; Przeworski KC; Chass GA Recycling the Waste: The Development of a Catalytic Wittig Reaction. Angew. Chem. Int. Ed 2009, 48, 6836–6839.

201. O'Brien CJ; Lavigne F; Coyle EE; Holohan AJ; Doonan BJ Breaking the Ring through a Room Temperature Catalytic Wittig Reaction. Chem. Eur. J 2013, 19, 5854–5858. [PubMed: 23526683]

202. Coyle EE; Doonan BJ; Holohan AJ; Walsh KA; Lavigne F; Krenske EH; O'Brien CJ Catalytic Wittig Reactions of Semi- and Nonstabilized Ylides Enabled by Ylide Tuning. Angew. Chem. Int. Ed 2014, 53, 585–12911.

203. Marinetti A; Carmichael D Synthesis and Properties of Phosphetanes. Chem. Rev 2002, 102, 201–230. [PubMed: 11782133]

204. Nykaza TV; Cooper JC; Radosevich AT anti-1,2,2,3,4,4-Hexamethylphosphetane 1-Oxide. Org. Synth 2019, 96, 418–435. [PubMed: 31902967]

205. Longwitz L; Spannenberg A; Werner T Phosphetane Oxides as Redox Cycling Catalysts in the Catalytic Wittig Reaction at Room Temperature. ACS Catal. 2019, 9, 9237–9244.

206. Hoffmann M; Deshmukh S; Werner T Scope and Limitation of the Microwave-Assisted Catalytic Wittig Reaction. Eur. J. Org. Chem 2015, 4532–4543.

207. Wang L; Sun M; Ding MW Catalytic Intramolecular Wittig Reaction Based on a Phosphine/Phosphine Oxide Catalytic Cycle for the Synthesis of Heterocycles. Eur. J. Org. Chem 2017, 2568–2578.

208. Burk MJ Modular Phospholane Ligands in Asymmetric Catalysis. Acc. Chem. Res 2000, 33, 363–372. [PubMed: 10891054]

209. Werner T; Hoffmann M; Deshmukh S First enantioselective catalytic Wittig reaction. Eur. J. Org. Chem 2014, 6630–6633.

210. Werner T; Hoffmann M; Deshmukh S Phospholane-Catalyzed Wittig Reaction. Eur. J. Org. Chem 2015, 3286–3295.

211. Schirmer M-LL; Adomeit S; Werner T First Base-Free Catalytic Wittig Reaction. Org. Lett 2015, 17, 3078–3081. [PubMed: 26020449]

212. Schirmer M-L; Adomeit S; Spannenberg A; Werner T Novel Base-Free Catalytic Wittig Reaction for the Synthesis of Highly Functionalized Alkenes. Chem. Eur. J 2016, 22, 2458–2465. [PubMed: 26762186]

213. Longwitz L; Werner T Reduction of Activated Alkenes by P^{III}/P^{V} Redox Cycling Catalysis. Angew. Chem. Int. Ed 2020, 59, 2760–2763..

214. Lee CJ; Chang TH; Yu JK; Madhusudhan Reddy G; Hsiao MY; Lin W Synthesis of Functionalized Furans via Chemoselective Reduction/Wittig Reaction Using Catalytic Triethylamine and Phosphine. Org. Lett 2016, 18, 3758–3761. [PubMed: 27434727]

215. Saleh N; Voituriez A Synthesis of 9*H*-Pyrrolo[1,2-*a*]indole and 3*H*-Pyrrolizine Derivatives via a Phosphine-Catalyzed Umpolung Addition/Intramolecular Wittig Reaction. J. Org. Chem 2016, 81, 4371–4377. [PubMed: 27080174]

216. Saleh N; Blanchard F; Voituriez A Synthesis of Nitrogen-Containing Heterocycles and Cyclopentenone Derivatives via Phosphine-Catalyzed Michael Addition/Intramolecular Wittig Reaction. Adv. Synth. Catal 2017, 359, 2304–2315.

217. Zhang K; Cai L; Yang Z; Houk KN; Kwon O Bridged [2.2.1] Bicyclic Phosphine Oxide Facilitates Catalytic γ-Umpolung Addition–Wittig Olefination. Chem. Sci 2018, 9, 1867–1872. [PubMed: 29732112]

218. Tsai YL; Lin W Synthesis of Multifunctional Alkenes from Substituted Acrylates and Aldehydes via Phosphine-Catalyzed Wittig Reaction. Asian J. Org. Chem 2015, 4, 1040–1043.

219. Lorton C; Castanheiro T; Voituriez A Catalytic and Asymmetric Process via P^{III}/P^{V}=O Redox Cycling: Access to (Trifluoromethyl)Cyclobutenes via a Michael Addition/Wittig Olefination Reaction. J. Am. Chem. Soc 2019, 141, 10142–10147. [PubMed: 31194912]

220. van Kalkeren HA; Bruins JJ; Rutjes FPJT; van Delft FL Organophosphorus-Catalysed Staudinger Reduction. Adv. Synth. Catal 2012, 354, 1417–1421.

221. Lenstra DC; Lenting PE; Mecinović J Sustainable Organophosphorus-Catalysed Staudinger Reduction. Green Chem. 2018, 20, 4418–4422.

222. Lenstra DC; Wolf JJ; Mecinović J Catalytic Staudinger Reduction at Room Temperature. J. Org. Chem 2019, 84, 6536–6545. [PubMed: 31050295]

223. Kosal AD; Wilson EE; Ashfeld BL Phosphine-Based Redox Catalysis in the Direct Traceless Staudinger Ligation of Carboxylic Acids and Azides. Angew. Chem. Int. Ed 2012, 51, 12036–12040.

224. Di Santo E; Alberto ME; Russo N; Toscano M Computational Investigation on the Mechanism of Amide Bond Formation by Using Phosphine-Based Redox Catalysis. ChemCatChem 2015, 7, 2309–2312.

225. Andrews KG; Denton RM A More Critical Role for Silicon in the Catalytic Staudinger Amidation: Silanes as Non-Innocent Reductants. Chem. Commun 2017, 53, 7982–7985.

226. White PB; Rijpkema SJ; Bunschoten RP; Mecinović J Mechanistic Insight into the Catalytic Staudinger Ligation. Org. Lett 2019, 21, 1011–1014. [PubMed: 30715895]

227. van Kalkeren HA; Te Grotenhuis C; Haasjes FS; Hommersom CA; Rutjes FPJT; van Delft FL Catalytic Staudinger/Aza-Wittig Sequence by in Situ Phosphane Oxide Reduction. Eur. J. Org. Chem 2013, 7059–7066.

228. Wang L; Wang Y; Chen M; Ding MW Reversible P(III)/P(V) Redox: Catalytic Aza-Wittig Reaction for the Synthesis of 4(3H)-Quinazolinones and the Natural Product Vasicinone. Adv. Synth. Catal 2014, 356, 1098–1104.

229. Wang L; Xie YB; Huang NY; Yan JY; Hu WM; Liu MG; Ding MW Catalytic aza-Wittig Reaction of Acid Anhydride for the Synthesis of 4*H*-Benzo[*d*][1,3]oxazin-4-ones and 4-Benzylidene-2-aryloxazol-5(4*H*)-ones. ACS Catal. 2016, 6, 4010–4016.

230. Lao Z; Toy PH Catalytic Wittig and Aza-Wittig Reactions. Beilstein J. Org. Chem 2016, 12, 2577–2587. [PubMed: 28144327]

231. Bel Abed H; Mammoliti O; Bande O; Van Lommen G; Herdewijn P Organophosphorus-Catalyzed Diaza-Wittig Reaction: Application to the Synthesis of Pyridazines. Org. Biomol. Chem 2014, 12, 7159–7166. [PubMed: 25101802]

232. Lertpibulpanya D; Marsden SP; Rodriguez-Garcia I; Kilner CA Asymmetric Aza-Wittig Reactions: Enantioselective Synthesis of β-Quaternary Azacycles. Angew. Chem. Int. Ed 2006, 45, 5000–5002.

233. Headley CE; Marsden SP Synthesis and Application of *P*-Stereogenic Phosphines as Superior Reagents in the Asymmetric Aza-Wittig Reaction J. Org. Chem 2007, 72, 7185–7189. [PubMed: 17713949]

234. Cai L; Zhang K; Chen S; Lepage RJ; Houk KN; Krenske EH; Kwon O Catalytic Asymmetric Staudinger–Aza-Wittig Reaction for the Synthesis of Heterocyclic Amines. J. Am. Chem. Soc 2019, 141, 9537–9542. [PubMed: 31184143]

235. Mukaiyama T Oxidation-Reduction Condensation. Angew. Chem. Int. Ed 1976, 15, 94–103.

236. Mukaiyama T Explorations into New Reaction Chemistry. Angew. Chem. Int. Ed 2004, 43, 5590–5614.

237. van Kalkeren HA; van Delft FL; Rutjes FPJT Catalytic Appel Reactions. Pure Appl. Chem 2012, 85, 817–828.

238. Hamstra DFJ; Lenstra DC; Koenders TJ; Rutjes FPJT; Mecinović J Poly(Methylhydrosiloxane) as a Green Reducing Agent in Organophosphorus-Catalysed Amide Bond Formation. Org. Biomol. Chem 2017, 15, 6426–6432. [PubMed: 28737181]

239. Longwitz L; Jopp S; Werner T Organocatalytic Chlorination of Alcohols by P(III)/P(V) Redox Cycling. J. Org. Chem 2019, 84, 7863–7870. [PubMed: 31135155]

240. Lenstra DC; Rutjes FPJT; Mecinović J Triphenylphosphine-Catalysed Amide Bond Formation between Carboxylic Acids and Amines. Chem. Commun 2014, 50, 5763–5766.

241. Denton RM; An J; Adeniran B Phosphine oxide-catalysed chlorination reactions of alcohols under Appel conditions. Chem. Commun 2010, 46, 3025–3027.

242. Denton RM; Tang X; Przeslak A Catalysis of Phosphorus(V)-Mediated Transformations: Dichlorination Reactions of Epoxides under Appel Conditions. Org. Lett 2010, 12, 4678–4681. [PubMed: 20845932]

243. Denton RM; An J; Adeniran B; Blake AJ; Lewis W; Poulton AM Catalytic Phosphorus(V)-Mediated Nucleophilic Substitution Reactions: Development of a Catalytic Appel Reaction. J. Org. Chem 2011, 76, 6749–6767. [PubMed: 21744876]

244. Denton RM; An J; Lindovska P; Lewis W Phosphonium salt-catalysed synthesis of nitriles from in situ activated oximes. Tetrahedron 2012, 68, 2899–2905.

245. An J; Tang X; Moore J; Lewis W; Denton RM Phosphorus(V)-catalyzed dichlorination reactions of aldehydes. Tetrahedron 2013, 69, 8769–8776.

246. Tang X; An J; Denton RM A procedure for Appel halogenations and dehydrations using a polystyrene supported phosphine oxide. Tetrahedron Lett. 2014, 55, 799–802.

247. Pongener I; Nikitin K; McGarrigle EM Synthesis of glycosyl chlorides using catalytic Appel conditions. Org. Biomol. Chem 2019, 17, 7531–7535. [PubMed: 31369028]

248. Jordan A; Denton RM; Sneddon HF Development of a More Sustainable Appel Reaction. ACS Sustain. Chem. Eng 2020, 8, 2300–2309.

249. Lecomte M; Lipshultz JM; Kim-Lee SH; Li G; Radosevich AT Driving Recursive Dehydration by P^{III}/P^{V} Catalysis: Annulation of Amines and Carboxylic Acids by Sequential C-N and C-C Bond Formation. J. Am. Chem. Soc 2019, 141, 12507–12512. [PubMed: 31345031]

250. O'Brien CJ (Univ. Texas, USA), Catalytic Wittig and Mitsunobu Reactions, US Patent 8901365, 2014.

251. Buonomo JA; Aldrich CC Mitsunobu Reactions Catalytic in Phosphine and a Fully Catalytic System. Angew. Chem. Int. Ed 2015, 54, 13041–13044.

252. Hirose D; Gazvoda M; Košmrlj J; Taniguchi T The "Fully Catalytic System" in Mitsunobu Reaction Has Not Been Realized Yet. Org. Lett 2016, 18, 4036–4039. [PubMed: 27481065]

253. Beddoe RH; Sneddon HF; Denton RM The catalytic Mitsunobu reaction: a critical analysis of the current state-of-the-art. Org. Biomol. Chem 2018, 16, 7774–7781. [PubMed: 30306184]

254. Beddoe RH; Andrews KG; Magné V; Cuthbertson JD; Saska J; Shannon-Little AL; Shanahan SE; Sneddon HF; Denton RM Redox-neutral organocatalytic Mitsunobu reaction. Science 2019, 365, 910–914. [PubMed: 31467220]

255. Harris JR; Haynes MT; Thomas AM; Woerpel KA Phosphine-Catalyzed Reductions of Alkyl Silyl Peroxides by Titanium Hydride Reducing Agents: Development of the Method and Mechanistic Investigations. J. Org. Chem 2010, 75, 5083–5091. [PubMed: 20604518]

256. Kirby AJ; Warren SG The Organic Chemistry of Phosphorus; Elsevier: Amsterdam, 1967; p 20.

257. Zhao W; Yan PK; Radosevich AT A Phosphetane Catalyzes Deoxygenative Condensation of α-Keto Esters and Carboxylic Acids via P^{III}/P^{V}=O Redox Cycling. J. Am. Chem. Soc 2015, 137, 616–619. [PubMed: 25564133]

258. Osman FH; El-Samahy FA Reactions of α-Diketones and *o*-Quinones with Phosphorus Compounds. Chem. Rev 2002, 102, 629–678. [PubMed: 11890753]

259. Bhattacharya AK; Thyagarajan G The Michaelis-Arbuzov Rearrangement. Chem. Rev 1981, 81, 415–430.

260. Cadogan JIG; Cameron-Wood M; Mackie RK; Searle RJG The Reactivity of Organophosphorus Compounds. Part XIX. Reduction of Nitro-Compounds by Triethyl Phosphite: A Convenient New Route to Carbazoles, Indoles, Indazoles, Triazoles, and Related Compounds. J. Chem. Soc 1965, 4831–4837.

261. Cadogan JIG Reduction of Nitro- and Nitroso-Compounds by Tervalent Phosphorus Reagents. Q. Rev. Chem. Soc 1968, 22, 222–251.

262. Cadogan JIG; Todd MJ Reduction of Nitro- and Nitroso-Compounds by Tervalent Phosphorus Reagents. Part IV. Mechanistic Aspects of the Reduction of 2,4,6-Trimethyl-2′-Nitrobiphenyl, 2-Nitrobiphenyl, and Nitrobenzene. J. Chem. Soc. C 1969, 2808–2813.

263. Armour M-A; Cadogan JIG; Grace DSB Reduction of Nitro- and Nitroso Compounds by Tervalent Phosphorus Reagents. Part XI. A Kinetic Study of the Effects of Varying the Reagent and the Nitro-Compound in the Conversion of *o*-Nitrobenzylideneamines to 2-Substituted Indazoles. J. Chem. Soc., Perkin Trans. 2 1975, 1185–1189.

264. Nykaza TV; Harrison TS; Ghosh A; Putnik RA; Radosevich AT A Biphilic Phosphetane Catalyzes N-N Bond-Forming Cadogan Heterocyclization via P^{III}/P^{V}=O Redox Cycling. J. Am. Chem. Soc 2017, 139, 6839–6842. [PubMed: 28489354]

265. Bickelhaupt FM; Houk KN Analyzing Reaction Rates with the Distortion/Interaction-Activation Strain Model. Angew. Chem. Int. Ed 2017, 56, 10070–10086.

266. Hawes W; Trippett S Steric Hindrance in the Alkaline Hydrolysis of Phosphinate Esters. Chem. Commun 1968, 577–578.

267. Corfield JR; De'ath NJ; Trippett S Displacement at Phosphorus in a Four-membered Ring. J. Chem. Soc. D 1970, 1502–1503.

268. Mislow K Role of Pseudorotation in the Stereochemistry of Nucleophilic Displacement Reactions. Acc. Chem. Res 1970, 3, 321–331.

269. Haake P; Ossip PS S_N1 Mechanisms in Displacement at Phosphorus. Solvolysis of Phosphinyl Chlorides. J. Am. Chem. Soc 1971, 93, 6924–6930.

270. Schoene J; Bel Abed H; Schmieder P; Christmann M; Nazaré M A General One-Pot Synthesis of 2H-Indazoles Using an Organophosphorus–Silane System. Chem. Eur. J 2018, 24, 9090–9100 [PubMed: 29644761]

271. Nykaza TV; Ramirez A; Harrison TS; Luzung MR; Radosevich AT Biphilic Organophosphorus-Catalyzed Intramolecular $C_{sp}2$–H Amination: Evidence for a Nitrenoid in Catalytic Cadogan Cyclizations. J. Am. Chem. Soc 2018, 140, 3103–3113. [PubMed: 29389114]

272. Tsao M-L; Gritsan N; James TR; Platz MS; Hrovat DA; Borden WT Study of the Chemistry of ortho- and para-Biphenylnitrenes by Laser Flash Photolysis and Time-Resolved IR Experiments and by B3LYP and CASPT2 Calculations. J. Am. Chem. Soc 2003, 125, 9343–9358 and references therein. [PubMed: 12889963]

273. Nykaza TV; Cooper JC; Li G; Mahieu N; Ramirez A; Luzung MR; Radosevich AT Intermolecular Reductive C–N Cross Coupling of Nitroarenes and Boronic Acids by P^{III}/P^{V}=O Catalysis. J. Am. Chem. Soc 2018, 140, 15200–15205. [PubMed: 30372615]

274. Li G; Qin Z; Radosevich ATP(III)/P(V)-Catalyzed Methylamination of Arylboronic Acids and Esters: Reductive C–N Coupling with Nitromethane as a Methylamine Surrogate. J. Am. Chem. Soc 2020, 142, 16205–16210. [PubMed: 32886500]

275. Li G; Nykaza TV; Cooper JC; Ramirez A; Luzung MR; Radosevich AT An Improved P^{III}/P^{V}=O-Catalyzed Reductive C-N Coupling of Nitroaromatics and Boronic Acids by Mechanistic Differentiation of Rate- And Product-Determining Steps. J. Am. Chem. Soc 2020, 142, 6786–6799. [PubMed: 32178514]

276. Li G; te Grotenhuis C; Radosevich AT Reductive Csp^2–N Coupling by P^{III}/P^{V}=O–Catalysis. Trends Chem. 2021, 3, 72.

277. Nykaza TV; Li G; Yang J; Luzung MR; Radosevich AT P^{III}/P^{V}=O Catalyzed Cascade Synthesis of *N*-Functionalized Azaheterocycles. Angew. Chem. Int. Ed 2020, 59, 4505–4510.

278. Ghosh A; Lecomte M; Kim-Lee SH; Radosevich AT Organophosphorus-Catalyzed Deoxygenation of Sulfonyl Chlorides: Electrophilic (Fluoroalkyl)Sulfenylation by P^{III}/P^{V}=O Redox Cycling. Angew. Chem. Int. Ed 2019, 58, 2864–2869.

279. Reichl KD; Dunn NL; Fastuca NJ; Radosevich AT Biphilic Organophosphorus Catalysis: Regioselective Reductive Transposition of Allylic Bromides via P^{III}/P^{V} Redox Cycling. J. Am. Chem. Soc 2015, 137, 5292–5295. [PubMed: 25874950]

280. Culley SA; Arduengo AJ Synthesis and structure of the first 10-P-3 species. J. Am. Chem. Soc 1984, 106, 1164–1165.

281. Arduengo AJ; Stewart CA; Davidson F; Dixon DA; Becker JY; Culley SA; Mizen MB The synthesis, structure, and chemistry of 10-Pn-3 systems: tricoordinate hypervalent pnicogen compounds. J. Am. Chem. Soc 1987, 109, 627–647.

282. Arduengo AJ; Stewart CA Low coordinate hypervalent phosphorus. Chem. Rev 1994, 94, 1215–1237.

283. Dunn NL; Ha M; Radosevich AT Main Group Redox Catalysis: Reversible P(III)/P(V) Redox Cycling at a Phosphorus Platform. J. Am. Chem. Soc 2012, 134, 11330–11333. [PubMed: 22746974]

284. Zeng G; Maeda S; Taketsugu T; Sakaki S Catalytic Transfer Hydrogenation by a Trivalent Phosphorus Compound: Phosphorus-Ligand Cooperation Pathway or P^{III}/P^{V} Redox Pathway? Angew. Chem. Int. Ed 2014, 53, 4633–4637.

285. Zeng G; Maeda S; Taketsugu T; Sakaki S Theoretical Study of Hydrogenation Catalysis of Phosphorus Compound and Prediction of Catalyst with High Activity and Wide Application Scope. ACS Catal. 2016, 6, 4859–4870.

286. Zeng G; Maeda S; Taketsugu T; Sakaki S Catalytic Hydrogenation of Carbon Dioxide with Ammonia-Borane by Pincer-Type Phosphorus Compounds: Theoretical Prediction. J. Am. Chem. Soc 2016, 138, 13481–13484. [PubMed: 27690395]

287. Ang HG; Lien WS Oxidative Addition of Substituted Arsines and Stibines with Bis(Trifluoromethyl)Nitroxyl. J. Fluor. Chem 1980, 15, 453–470.

288. Smith MD Product Class 1: Arsenic Compounds. In Science of Synthesis: Organometallics; Fleming I, Ed.; Thieme: Stuttgart, 2002; Vol. 4, pp 13–51.

289. Gosney I; Lillie TJ; Lloyd D Reaction of Arsonium Ylides with Carbonyl Compounds—Effect of Substituents at Arsenic. Angew. Chem. Int. Ed 1977, 16, 487–488.

290. Lloyd D; Gosney I; Ormiston RA Arsonium Ylides (with some mention also of Arsinimines, Stibonium and Bismuthonium ylides). Chem. Soc. Rev 1987, 16, 45–74.

291. Aggarwal VK; Patel M; Studley J Synthesis of epoxides from aldehydes and tosylhydrazone salts catalysed by triphenylarsine: Complete *trans* selectivity for all combinations of coupling partners. Chem. Commun 2002, 1514–1515.

292. Zhu S; Liao Y; Zhu S Transition-Metal-Catalyzed Formation of *trans* Alkenes via Coupling of Aldehydes. Org. Lett 2004, 6, 377–380. [PubMed: 14748597]

293. Hellwinkel D; Knabe B Eliminierungen Und Umlagerungen Bei Alkyl- Und Alkenyl-bis-2.2′-biphenylylen-arsenen. Chem. Ber 1971, 104, 1761–1782.

294. Ciganek E Negatively Substituted Acetylenes. III. Reverse Wittig Reactions with Triphenylphosphine Oxide and Triphenylarsine Oxide. J. Org. Chem 1970, 35, 1725–1729.

295. Lu X-Y; Wang Q-W; Tao X-C; Sun J-H; Lei G-X Novel methods for the deoxygenation of triphenylarsine oxide to triphenylarsine. Acta Chim. Sinica 1985, 3, 337–341.

296. Shi L; Wang W; Wang Y; Huang YZ The First Example of a Catalytic Wittig-Type Reaction. Tri-*n*-Butylarsine-Catalyzed Olefination in the Presence of Triphenyl Phosphite. J. Org. Chem 1989, 54, 2027–2028.

297. Inaba R; Kawashima I; Fujii T; Yumura T; Imoto H; Naka K Systematic Study on the Catalytic Arsa-Wittig Reaction. Chem. Eur. J 2020, 26, 13400–13407. [PubMed: 32662545]

298. Cao P; Li CY; Kang YB; Xie Z; Sun XL; Tang Y Ph_3As-Catalyzed Wittig-Type Olefination of Aldehydes with Diazoacetate in the Presence of $Na_2S_2O_4$. J. Org. Chem 2007, 72, 6628–6630. [PubMed: 17655362]

299. Wang P; Liu CR; Sun XL; Chen SS; Li JF; Xie Z; Tang Y A Newly-Designed PE-Supported Arsine for Efficient and Practical Catalytic Wittig Olefination. Chem. Commun 2012, 48, 290–292.

300. Akiba K Mechanism of ligand coupling of hypervalent pentaarylantimony compounds. Pure Appl. Chem 1996, 68, 837–842.

301. Huang Y Synthetic Applications of Organoantimony Compounds. Acc. Chem. Res 1992, 25, 182–187.

302. Huang Y; Shen Y; Chen C Bromodiphenylstibine-Mediated Oxidation of Benzyl Alcohols by Bromine. Synthesis 1985, 651–652.

303. Akiba K; Ohnari H; Ohkata K Oxidation of α-Hydroxyketones with Triphenylantimony Dibromide and its Catalytic Cycle. Chem. Lett 1985, 14, 1577–1580.

304. Yasukie S; Koshi Y; Kawara S; Kurita J Catalytic Action of Triarylstibanes: Oxidation of Benzoins into Benzyls using Triarylstibanes under an Aerobic Condition. Chem. Pharm. Bull 2005, 53, 425–427.

305. Zhang W; Shi M Reduction of activated carbonyl groups by alkyl phosphines: Formation of α-hydroxy esters and ketones. Chem. Commun 2006, 1218–1220.

306. Wei Y; Liu X-G; Shi M Reduction of Activated Carbonyl Groups using Alkylphosphanes as Reducing Agents: A Mechanistic Study. Eur. J. Org. Chem 2012, 2386–2393.

307. Miller EJ; Zhao W; Herr JD; Radosevich AT A Nonmetal Approach to α-Heterofunctionalized Carbonyl Derivatives by Formal Reductive X–H Insertion. Angew. Chem. Int. Ed 2012, 51, 10605–10609.
308. Zhao W; Fink DM; Labutta CA; Radosevich AT A $C_{sp}3$–$C_{sp}3$ Bond Forming Reductive Condensation of α-Keto Esters and Enolizable Carbon Pronucleophiles. Org. Lett 2013, 15, 3090–3093. [PubMed: 23738614]
309. Hutchins EB Jr.; Lenher V Pentavalent Bismuth. J. Am. Chem. Soc 1907, 29, 31–33.
310. Barton DHR; Lester DJ; Motherwell WB; Papoula MTB Oxidation of Organic Substrates by Pentavalent Organobismuth Reagents. J. Chem. Soc., Chem Commun 1979, 705–707.
311. Barton DHR; Kitchin JP; Lester DJ; Motherwell WB; Papoula MTB Functional Group Oxidation by Pentavalent Organobismuth Reagents. Tetrahedron 1981, 37, 73–79.
312. Jurrat M; Maggi L; Lewis W; Ball LT Modular bismacycles for the selective C–H arylation of phenols and naphthols. Nature Chem. 2020, 12, 260–269. [PubMed: 32108765]
313. Šimon P; De Proft F; Jambor R; Růžička A; Dostál L Monomeric Organoantimony(I) and Organobismuth(I) Compounds Stabilized by an NCN Chelating Ligand: Syntheses and Structures. Angew. Chem. Int. Ed 2010, 49, 5468–5471.
314. Vránová I; Alonso M; Lo R; Sedlák R; Jambor R; Růžička A; De Proft F; Hobza P; Dostál L From Dibismuthenes to Three- and Two-Coordinated Bismuthinidenes by Fine Ligand Tuning: Evidence for Aromatic BiC_3N Rings through a Combined Experimental and Theoretical Study. Chem. Eur. J 2015, 21, 16917–16928. [PubMed: 26434943]
315. Šimon P; Jambor R; Růžička A; Dostál L Oxidative addition of organic disulfides to low valent *N,C,N*-chelated organobismuth(I) compound: Isolation, structure and coordination capability of substituted bismuth(III) bis(arylsulfides). J. Organomet. Chem 2013, 740, 98–103.
316. Šimon P; Jambor R; Růžička A; Dostál L Oxidative Addition of Diphenyldichalcogenides PhEEPh (E = S, Se, Te) to Low-Valent CN- and NCN-Chelated Organoantimony and Organobismuth Compounds. Organometallics 2013, 32, 239–248.
317. Hejda M; Jirásko R; Růžička A; Jambor R; Dostál L Probing the Limits of Oxidative Addition of C(sp^3)–X Bonds toward Selected *N,C,N*-Chelated Bismuth(I) Compounds. Organometallics 2020, 39, 4320–4328.
318. Ishida S; Hirakawa F; Furukawa K; Yoza K; Iwamoto T Persistent Antimony- and Bismuth-Centered Radicals in Solution. Angew. Chem. Int. Ed 2014, 53, 11172–11176.
319. Schwamm RJ; Harmer JR; Lein M; Fitchett CM; Granville S; Coles MP Isolation and Characterization of a Bismuth(II) Radical. Angew. Chem. Int. Ed 2015, 54, 10630–10633.
320. Callahan JL; Grasselli RK; Milberger EC; Strecker HA Oxidation and Ammoxidation of Propylene over Bismuth Molybdate Catalyst. Ind. Eng. Chem. Prod. Res. Dev 1970, 9, 134–142.
321. Pudar S; Oxgaard J; Goddard WA III. Mechanism of Selective Ammoxidation of Propene to Acrylonitrile on Bismuth Molybdates from Quantum Mechanical Calculations. J. Phys. Chem. C 2010, 114, 15678–15694.
322. Licht RB; Bell AT A DFT Investigation of the Mechanism of Propene Ammoxidation over α-Bismuth Molybdate. ACS Catal. 2017, 7, 161–176.
323. Perlin AS Glycol-Cleavage Oxidation. In Adv. Carbohydr. Chem. Biochem Horton D, Ed.; Academic Press: 2006; Vol. 60, pp 183–250. [PubMed: 16750444]
324. Zevaco T; Duñach E; Postel M Bi(III)-mandelate/DMSO: A New Oxidizing System for the Catalyzed C-C Cleavage of Epoxides. Tetrahedron Lett. 1993, 34, 2601–2604.
325. Le Boisselier V; Duñach E; Postel M Bismuth(III)-catalyzed oxidative cleavage of aryl epoxides: substituent effects on the kinetics of the oxidation reaction. J. Organomet. Chem 1994, 482, 119–123.
326. Le Boisselier V; Coin C; Postel M; Duñach E Molecular Oxygen Oxidative Carbon-Carbon Bond Cleavage of α-Ketols Catalyzed by Bi(III) Carboxylates. Tetrahedron 1995, 51, 4991–4996.
327. Antoniotti S; Duñach E Novel and catalytic oxidation of internals epoxides to α-diketones. Chem. Commun 2001, 2566–2567.
328. Favier I; Duñach E Oxidation of mandelic acid derivatives catalysed by $Bi(0)/O_2$ systems: mechanistic considerations. Tetrahedron 2003, 59, 1823–1830.

329. Antoniotti S; Duñach E Mechanistic Aspects of the Bismuth-Catalysed Oxidation of Epoxides to α-Diketones. Eur. J. Org. Chem 2004, 3459–3464.
330. Salvador JAR; Silvestre SM Bismuth-catalyzed allylic oxidation using *t*-butyl hydroperoxide. Tetrahedron Lett. 2005, 46, 2581–2584.
331. Bonvin Y; Callens E; Larrosa I; Henderson DA; Oldham J; Burton AJ; Barrett AGM Bismuth-Catalyzed Benzylic Oxidations with *tert*-Butyl Hydroperoxide. Org. Lett 2005, 7, 4549–4552. [PubMed: 16209476]
332. Callens E; Burton AJ; White AJP; Barrett AGM Mechanistic study on benzylic oxidations catalyzed by bismuth(III) salts: X-ray structures of two bismuth-picolinate complexes. Tetrahedron Lett. 2008, 49, 3709–3712.
333. Schwamm RJ; Lein M; Coles MP; Fitchett CM Catalytic oxidative coupling promoted by bismuth TEMPOxide complexes. Chem. Commun 2018, 54, 916–919.
334. Ramler J; Krummenacher I; Lichtenberg C &Homogeneous Catalysis Well-Defined, Molecular Bismuth Compounds: Catalysts in Photochemically Induced Radical Dehydrocoupling Reactions. Chem. Eur. J 2020, 26, 14551–14555. [PubMed: 32573876]
335. Shimada S, Rao MLN Transition-Metal Catalyzed C–C Bond Formation Using Organobismuth Compounds. Top. Curr. Chem 2012, 311, 199–228. [PubMed: 21809192]
336. Planas O; Wang F; Leutzsch M; Cornella J Flourination of arylboronic esters enabled by bismuth redox catalysis. Science 2020, 317, 313–317. [PubMed: 31949081]
337. Planas O; Peciukenas V; Cornella J Bismuth-Catalyzed Oxidative Coupling of Arylboronic Acids with Triflate and Nonaflate Salts. J. Am. Chem. Soc 2020, 142, 11382–11387. [PubMed: 32536157]
338. Wang F; Planas O; Cornella J Bi(I)-Catalyzed Transfer-Hydrogenation with Ammonia-Borane. J. Am. Chem. Soc 2019, 141, 4235–4240. [PubMed: 30816708]
339. Pang Y; Leutzsch M; Nöthling N; Cornella J Catalytic Activation of N_2O at a Low-Valent Bismuth Redox Platform. J. Am. Chem. Soc 2020, 142, 19473–19479. [PubMed: 33146996]
340. Cowley AH; Kemp RA Synthesis and Reaction Chemistry of Stable Two-Coordinate Phosphorus Cations (Phosphenium Ions). Chem. Rev 1985, 85, 367–382.
341. Dostál L Quest for stable or masked pnictinidenes: Emerging and exciting class of group 15 compounds. Coord. Chem. Rev 2017, 353, 142–158.
342. Doyle AG; Jacobsen EN Small-Molecule H-Bond Donors in Asymmetric Catalysis. Chem. Rev 2007, 107, 5713–5743. [PubMed: 18072808]
343. Phipps RJ; Hamilton GL; Toste FD The Progression of Chiral Anions from Concepts to Applications in Asymmetric Catalysis. Nat. Chem 2012, 4, 603–614. [PubMed: 22824891]
344. Brak K; Jacobsen EN Asymmetric Ion-Pairing Catalysis. Angew. Chem. Int. Ed 2013, 52, 534–561.
345. Mahlau M; List B Asymmetric Counteranion-Directed Catalysis: Concept, Definition, and Applications. Angew. Chem. Int. Ed 2013, 52, 518–533.
346. Wang T; Han X; Zhong F; Yao W; Lu Y Amino Acid-Derived Bifunctional Phosphines for Enantioselective Transformations. Acc. Chem. Res 2016, 49, 1369–1378. [PubMed: 27310293]
347. Bruggink A; Schoevaart R; Kieboom T Concepts of Nature in Organic Synthesis: Cascade Catalysis and Multistep Conversions in Concert. Org. Process Res. Dev 2003, 7, 622–640.
348. Fogg DE; Dos Santos EN Tandem Catalysis: A Taxonomy and Illustrative Review. Coord. Chem. Rev 2004, 248, 2365–2379.
349. Wasilke JC; Obrey SJ; Baker RT; Bazan GC Concurrent Tandem Catalysis. Chem. Rev 2005, 105, 1001–1020. [PubMed: 15755083]
350. Shindoh N; Takemoto Y; Takasu K Auto-Tandem Catalysis: A Single Catalyst Activating Mechanistically Distinct Reactions in a Single Reactor. Chem. Eur. J 2009, 15, 12168–12179. [PubMed: 19847824]
351. Lohr TL; Marks TJ Orthogonal Tandem Catalysis. Nat. Chem 2015, 7, 477–482. [PubMed: 25991525]
352. Allen AE; MacMillan DWC Synergistic Catalysis: A Powerful Synthetic Strategy for New Reaction Development. Chem. Sci 2012, 3, 633–658.

353. Prier CK; Rankic DA; MacMillan DWC Visible Light Photoredox Catalysis with Transition Metal Complexes: Applications in Organic Synthesis. Chem. Rev 2013, 113, 5322–5363. [PubMed: 23509883]

354. Studer A; Curran DP The Electron Is a Catalyst. Nat. Chem 2014, 6, 765–773. [PubMed: 25143210]

355. Staveness D; Bosque I; Stephenson CRJ Free Radical Chemistry Enabled by Visible Light-Induced Electron Transfer. Acc. Chem. Res 2016, 49, 2295–2306. [PubMed: 27529484]

356. Shaw MH; Twilton J; MacMillan DWC Photoredox Catalysis in Organic Chemistry. J. Org. Chem 2016, 81, 6898–6926. [PubMed: 27477076]

357. Yan M; Lo JC; Edwards JT; Baran PS Radicals: Reactive Intermediates with Translational Potential. J. Am. Chem. Soc 2016, 138, 12692–12714. [PubMed: 27631602]

358. Yan M; Kawamata Y; Baran PS Synthetic Organic Electrochemical Methods since 2000: On the Verge of a Renaissance. Chem. Rev 2017, 117, 13230–13319. [PubMed: 28991454]

359. Smith JM; Harwood SJ; Baran PS Radical Retrosynthesis. Acc. Chem. Res 2018, 51, 1807–1817. [PubMed: 30070821]

360. Bentrude WG The Chemistry of Organophosphorus Compounds; Hartley FR, Ed.; Wiley: Chichester, 1990; Vol. 1, pp 531–566.

361. Marque S; Tordo P Reactivity of Phosphorus Centered Radicals. Top. Curr. Chem 2005, 250, 43–76.

362. Yasui S; Shioji K; Ohno A; Yoshihara M Reactivity of Phosphorus-Centered Radicals Generated during the Photoreaction of Diphenylphosphinous Acid with 10-Methylacridinium Salt. J. Org. Chem 1995, 60, 2099–2105.

363. Nakamura M; Miki M; Majima T Substituent Effect on the Photoinduced Electron-Transfer Reaction of Para-Substituted Triphenylphosphines Sensitised by 9,10-Dicyano-Anthracene. J. Chem. Soc. Perkin Trans. 2 2000, 7, 1447–1452.

364. Ohkubo K; Nanjo T; Fukuzumi S Photocatalytic Electron-Transfer Oxidation of Triphenylphosphine and Benzylamine with Molecular Oxygen via Formation of Radical Cations and Superoxide Ion. Bull. Chem. Soc. Jpn 2006, 79, 1489–1500.

365. Yasui S; Tojo S; Majima T Effects of Substituents on Aryl Groups during the Reaction of Triarylphosphine Radical Cation and Oxygen. Org. Biomol. Chem 2006, 4, 2969–2973. [PubMed: 16855746]

366. Yasui S; Tsujimoto M Investigation of Non-Rehm-Weller Kinetics in the Electron Transfer from Trivalent Phosphorus Compounds to Singlet Excited Sensitizers. J. Phys. Org. Chem 2013, 26, 1090–1097.

367. Zhang Y; Ye C; Li S; Ding A; Gu G; Guo H Eosin Y-Catalyzed Photooxidation of Triarylphosphines under Visible Light Irradiation and Aerobic Conditions. RSC Adv. 2017, 7, 13240–13243.

368. Kargin YM; Budnikova YG Electrochemistry of organophosphorus compounds. Russ. J. Gen. Chem 2001, 71, 1393.

369. Shao X; Zheng Y; Ramadoss V; Tian L; Wang Y Recent Advances in P^{III}-Assisted Deoxygenative Reactions under Photochemical or Electrochemical Conditions. Org. Biomol. Chem 2020, 18, 5994–6005. [PubMed: 32692327]

370. Complexes of Sb and Bi with redox-active ligands, particularly porphyrins, have been used as photocatalysts and photosensitizers (Refs. 371-375) as well as electrocatalysts (Refs. 376-377).

371. Kalyanasundaram K; Shelnutt JA; Grätzel M Sensitization and Photoredox Reactions of Zinc(II) and Antimony(V) Uroporphyrins in Aqueous Media. Inorg. Chem 1988, 27, 2820–2825.

372. Knör G; Vogler A Photochemistry and Photophysics of Antimony(III) *Hyper* Porphyrins: Activation of Dioxygen Induced by a Reactive sp Excited State. Inorg. Chem 1994, 33, 314–318.

373. Knör G; Vogler A; Roffia S; Paolucci F; Balzani V Switchable photoreduction pathways of antimony(v) tetraphenylporphyrin. A potential multielectron transfer photosensitizer. Chem. Commun 1996, 1643–1644.

374. Shiragami T; Matsumoto J; Inoue H; Yasuda M Antimony porphyrin complexes as visible-light driven photocatalyst. J. Photochem. Photobiol. C 2005, 6, 227–248.

375. Ertl M; Wöß E; Knör G Antimony porphyrins as red-light powered photocatalysts for solar fuel production from halide solutions in the presence of air. Photochem. Photobiol. Sci. 2015, 14, 1826–1830. [PubMed: 26360604]

376. Jiang J;Materna KL; Hedström S;Yang KR; Crabtree RH; Batista VS; Brudvig GW Antimony Complexes for Electrocatalysis: Activity of a Main-Group Element in Proton Reduction. Angew. Chem. Int. Ed 2017, 56, 9111–9115.

377. Xiao W-C; Tao Y-W; Luo G-G Hydrogen formation using a synthetic heavier main-group bismuth-based electrocatalyst. Int. J. Hydrog. Energy 2020, 45, 8177–8185.

378. Pan D; Nie G; Jiang S; Li T; Jin Z Radical reactions promoted by trivalent tertiary phosphines. Org. Chem. Front 2020, 7, 2349–2371.

379. Stache ER; Ertel AB; Rovis T; Doyle AG Generation of Phosphoranyl Radicals via Photoredox Catalysis Enables Voltage–Independent Activation of Strong C–O Bonds. ACS Catal. 2018, 8, 11134–11139. [PubMed: 31367474]

380. Fedorov OV; Scherbinina SI; Levin VV; Dilman AD Light-Mediated Dual Phosphine-/Copper-Catalyzed Atom Transfer Radical Addition Reaction. J. Org. Chem 2019, 84, 11068–11079. [PubMed: 31409063]

381. Martinez Alvarado JI; Ertel A,B; Stegner A; Stache EE; Doyle AG Direct Use of Carboxylic Acids in the Photocatalytic Hydroacylation of Styrenes to Generate Dialkyl Ketones. Org. Lett 2019, 21, 9940–9944. [PubMed: 31750667]

382. Rossi-Ashton JA; Clarke AK; Unsworth WP; Taylor RJK Phosphoranyl Radical Fragmentation Reactions Driven by Photoredox Catalysis. ACS Catal. 2020, 10, 7250–7261. [PubMed: 32905246]

383. Manabe S; Wong CM; Sevov CS Direct and Scalable Electroreduction of Triphenylphosphine Oxide to Triphenylphosphine. J. Am. Chem. Soc 2020, 142, 3024–3031. [PubMed: 31948233]

384. Chakraborty B; Kostenko A; Menezes PW; Driess M A Systems Approach to a One-Pot Electrochemical Wittig Olefination Avoiding the Use of a Chemical Reductant or Sacrificial Electrode. Chem. Eur. J 2020, 26, 11829–11834. [PubMed: 32259335]

385. Charaborty B; Menezes PW; Driess M Beyond CO_2 Reduction: Vistas on Electrochemical Reduction of Heavy Non-metal Oxides with Very Strong E–O Bonds (E = Si, P, S). J. Am. Chem. Soc 2020, 142, 14772–14788. [PubMed: 32786773]

386. Elias JS; Costentin C; Nocera DG Direct Electrochemical P(V) to P(III) Reduction of Phosphine Oxide Facilitated by Triaryl Borates. J. Am. Chem. Soc 2018, 140, 13711–13718. [PubMed: 30278122]

387. Martínez-Calvo M; Mascareñas JL Organometallic Catalysis in Biological Media and Living Settings. Coord. Chem. Rev 2018, 359, 57–79.

388. Vantourout JC; Adusumalli SR; Knouse KW; Flood DT; Ramirez A; Padial NM; Istrate A; Maziarz K; deGruyter JN; Merchant RR; Qiao JX; Schmidt MA; Deery MJ; Eastgate MD; Dawson PE; Bernardes GJL; Baran PS Serine-Selective Bioconjugation. J. Am. Chem. Soc 2020, 142, 17236–17242. [PubMed: 32965106]

389. A similar question was framed by a reviewer of this Perspective: “What outstanding problem[s] in chemical catalysis will be solved by all of this effort?”.

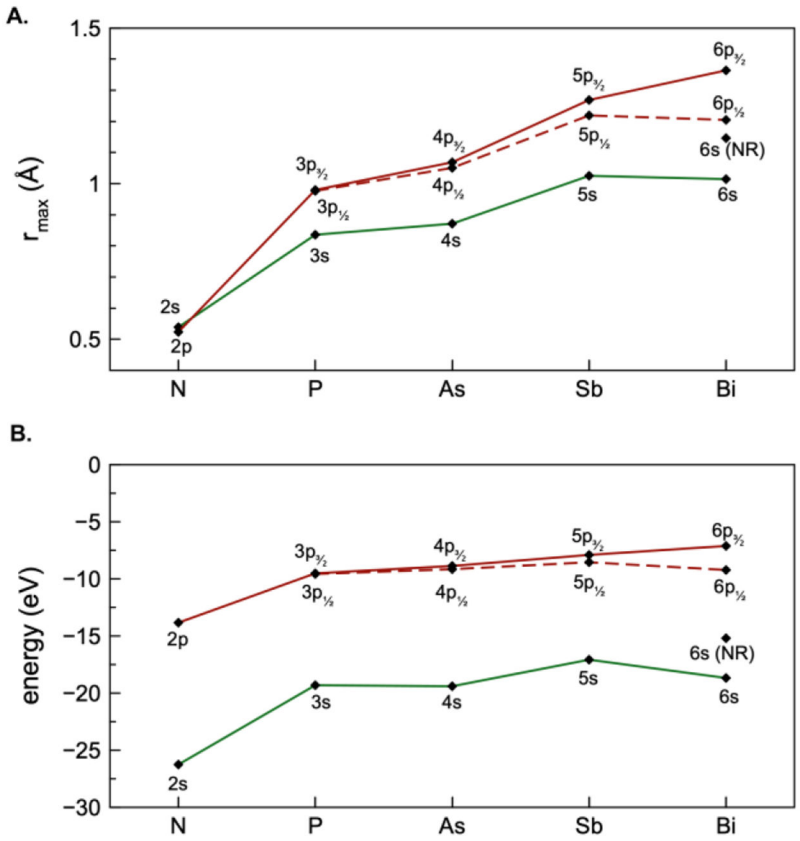

Figure 1.

(A) Atomic orbital radial probability function of Group 15 elements. (B) Valence atomic orbital 1-electron ionization energies of Group 15 elements.

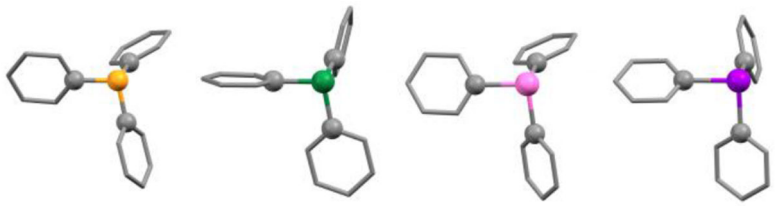

	PPh_3	$AsPh_3$	$SbPh_3$	$BiPh_3$
$d_{Pn–C}$ (Å)	1.93	1.96	2.15	2.25
<(C–Pn–C)	102.7°	100.4°	96.6°	93.7°
E_{inv} (PnH_3) (kcal/mol)	35.1	39.2	43.9	63.1

Figure 2.

(*top*) Solid-state structures for Ph_3Pn (Pn = P, As, Sb, Bi) viewed orthonormal to one of the equivalent C_α-Pn-C_α' planes. Periodic variation in bond angles and pyramidalization are thereby best visualized. (bottom) Tabulated structural data for Ph_3Pn, and computed inversion barriers of PnH_3.

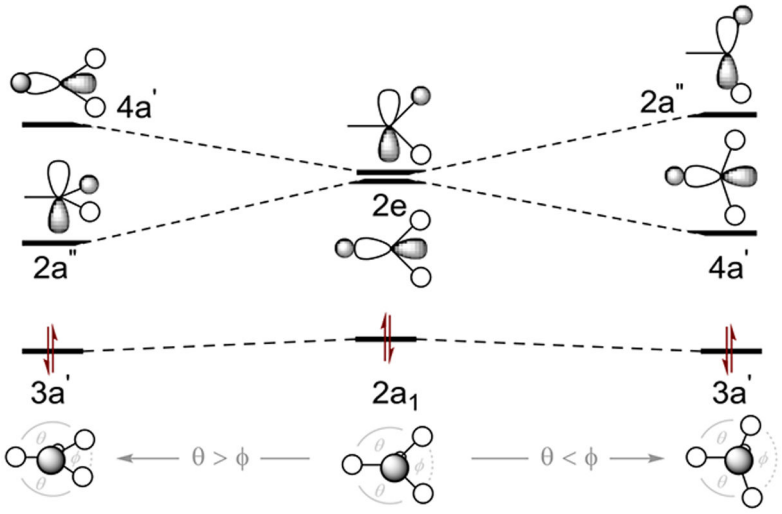

Figure 3.

Qualitative correlation diagram for frontier orbitals in C_{3v} symmetry (center) upon descent to C_s symmetry (left and right). Orbital projections are viewed down the σ plane.

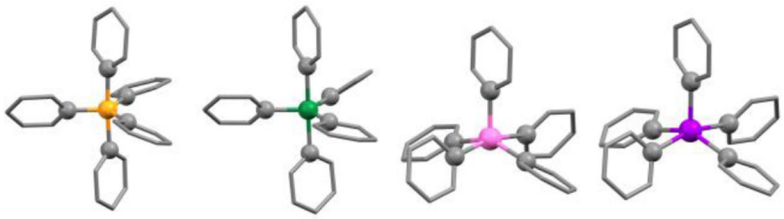

	PPh_5	$AsPh_5$	$SbPh_5$	$BiPh_5$
$d_{Pn-C_{eq}}$(Å)	1.85	1.97	2.22	2.32
$d_{Pn-C_{ax}}$(Å)	1.99	2.10	2.13	2.23
τ	0.90	0.98	0.25	0.22

Figure 4.
Solid-state structures and structural data of Ph_5Pn.

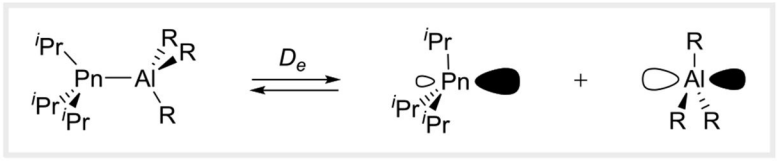

R = H | R = ^{t}Bu

P	As	Sb	Bi		P	As	Sb	Bi
2.58	2.66	2.90	2.99	d(Pn–Al) (Å)	3.38	3.68	3.53	3.67
22.3	17.7	13.6	10.3	D_e (kcal/mol)	2.6	4.0	4.1	3.0

Figure 5.

Gas-phase Pn–Al distances and dissociation enthalpies (D_e) of Lewis adducts $H_3Al–Pn^iPr_3$ and $^tBu_3Al–Pn^iPr_3$.

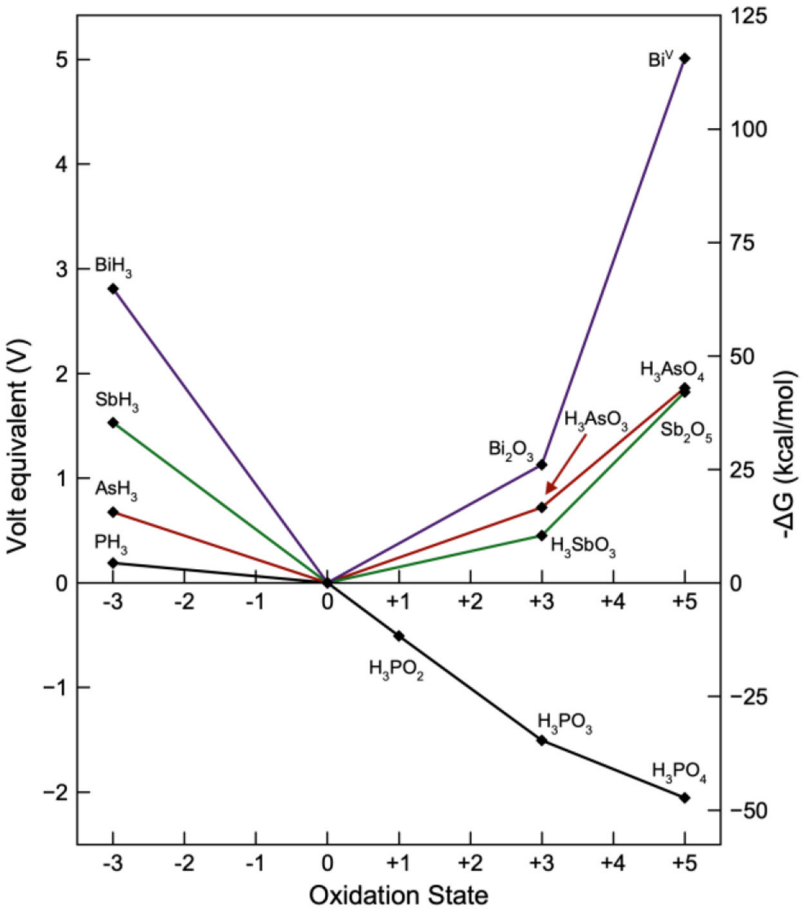

Figure 6.
Frost oxidation state diagram for heavier pnictogens under acidic conditions.

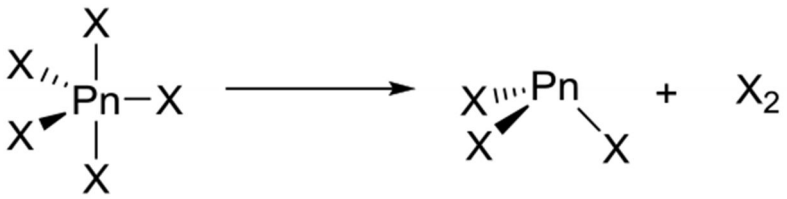

ΔG_{rxn}	P	As	Sb	Bi
X = H	–45.3	–54.6	–50.2	–73
X = F	158.1	126.9	125.5	79.7

Figure 7.
Gas-phase energies (kcal/mol) for the reactions $PnF_5 \rightarrow PnF_3 + F_2$ and $PnH_5 \rightarrow PnH_3 + H_2$.

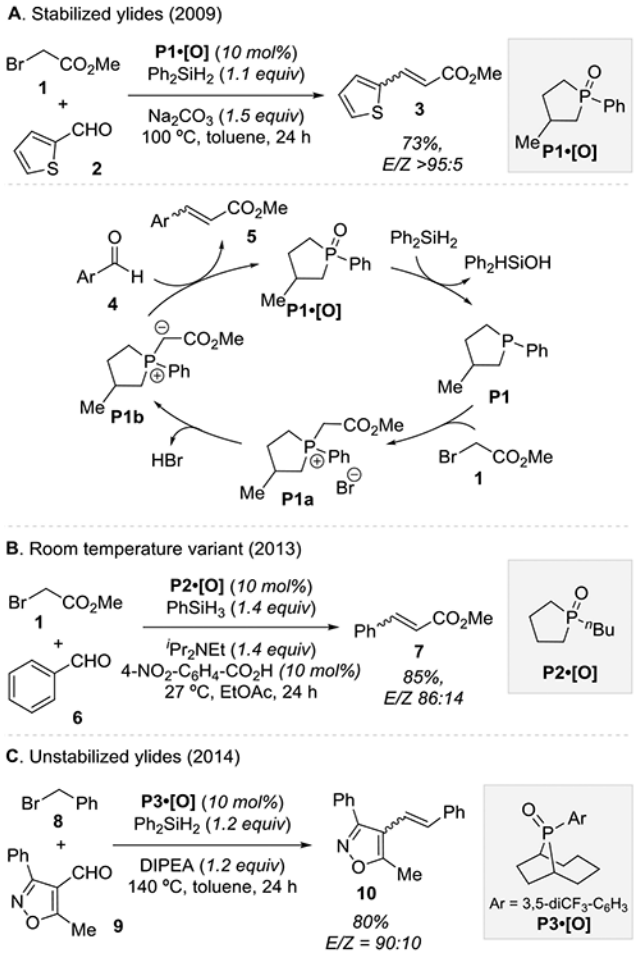

Figure 8.

Phospholane-catalyzed Wittig reaction with (A) stabilized ylides and mechanism, (B) stabilized ylides at ambient temperature through inclusion of Brønsted acid additive, and (C) unstabilized ylides through development of electron-deficient phospholane catalyst.

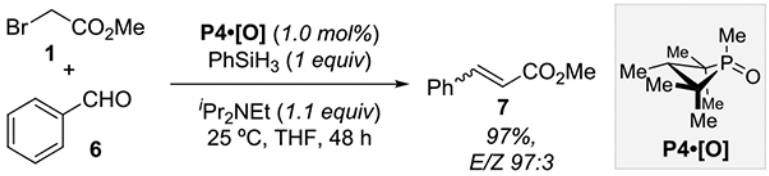

Figure 9.
Phosphetane-catalyzed Wittig reaction with stabilized ylides at ambient temperature.

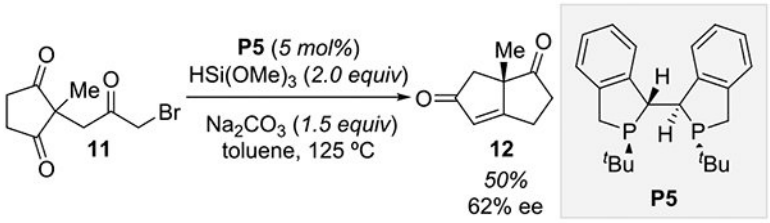

Figure 10.
Chiral phospholane-catalyzed asymmetric Wittig cyclization.

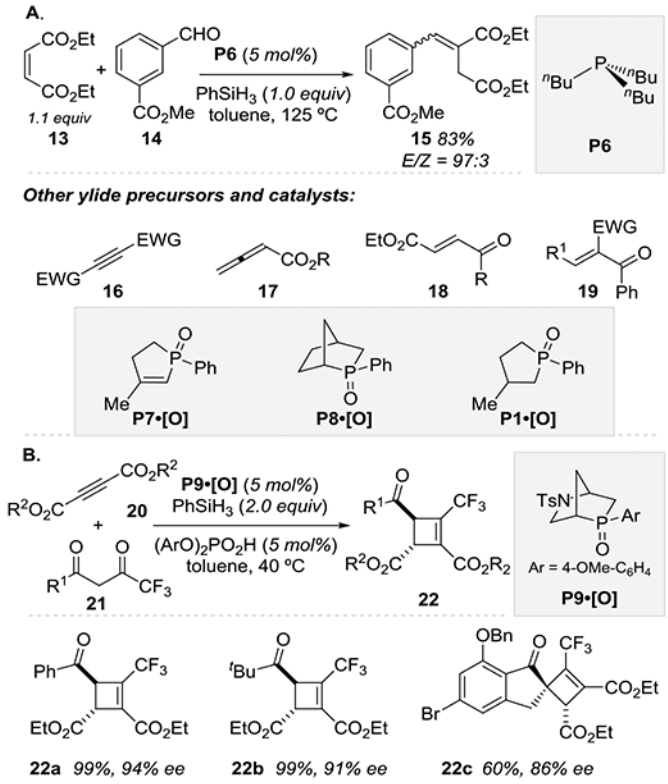

Figure 11.

A) Catalytic Wittig reactions from unsaturated ylide precursors. B) Asymmetric organophosphorus-catalyzed (trifluoromethyl)cyclobutene formation via a conjugate addition/Wittig olefination reaction.

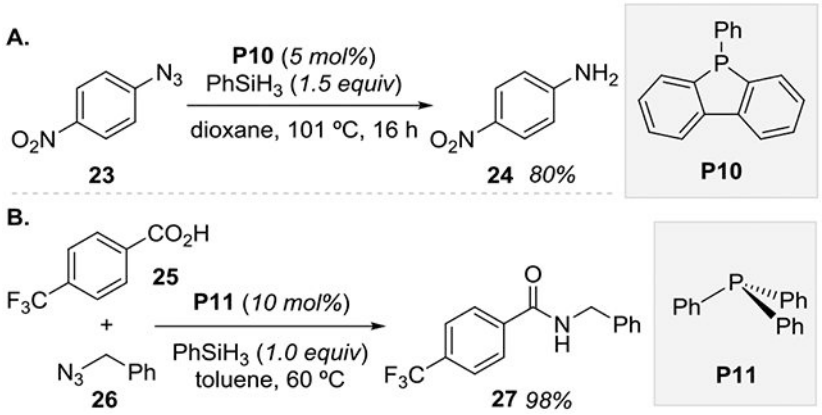

Figure 12.

A) Dibenzophosphole-catalyzed Staudinger reduction. B) PPh_3-catalyzed Staudinger ligation.

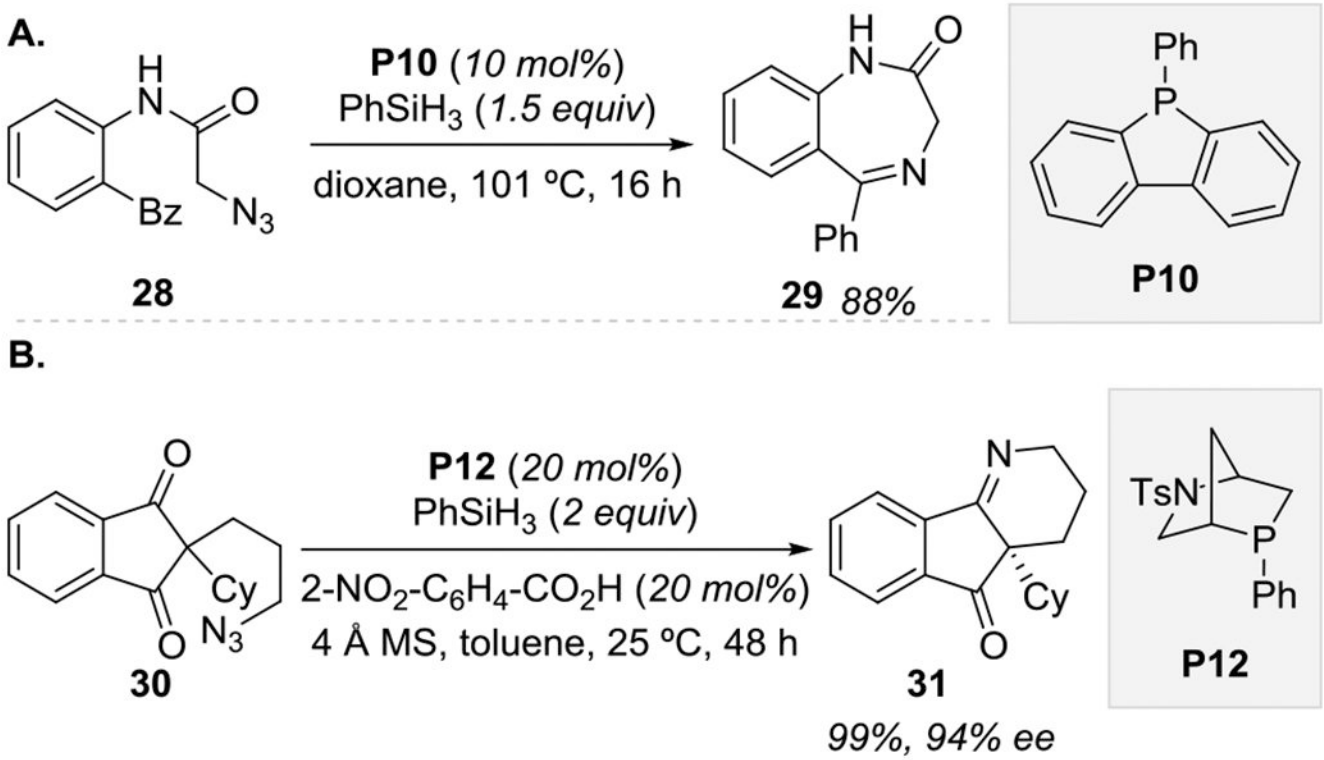

Figure 13.

A) Catalytic aza-Wittig reactions using benzo[*b*]phosphindole. B) Catalytic enantioselective aza-Wittig synthesis of chiral heterocycles catalyzed by HypPhos. Bz = benzoyl; Cy = cyclohexyl; Ts = tosyl.

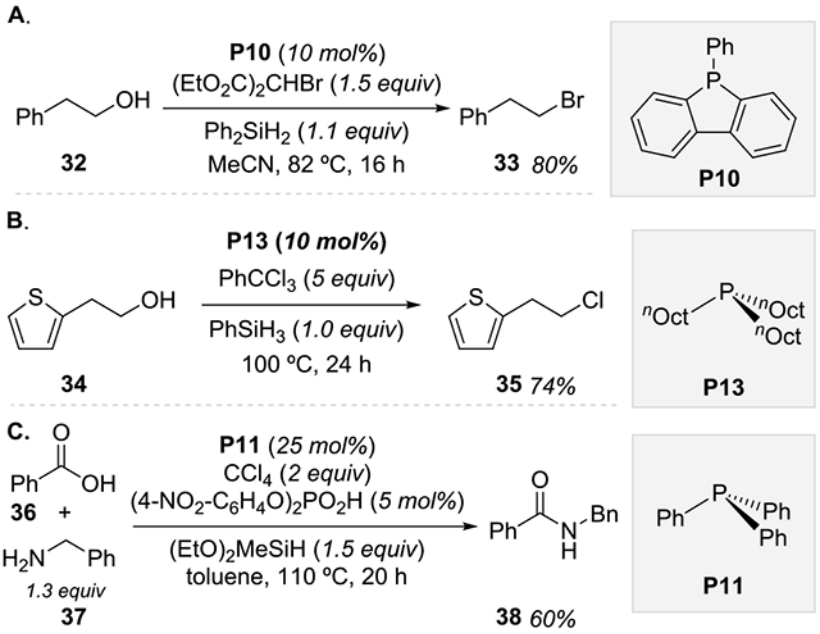

Figure 14.

Organophosphorus-catalyzed Appel A) bromination, B) chlorination, and C) amidation. Bn = benzyl.

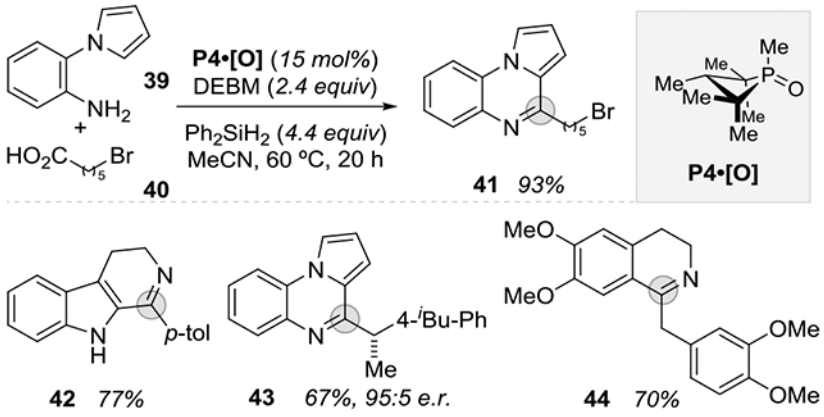

Figure 15.

Phosphetane-catalyzed tandem annulation of amines and carboxylic acids by sequential C–N and C–C bond formation. *p*-tol = *para*-tolyl; ^{i}Bu = *iso*-butyl.

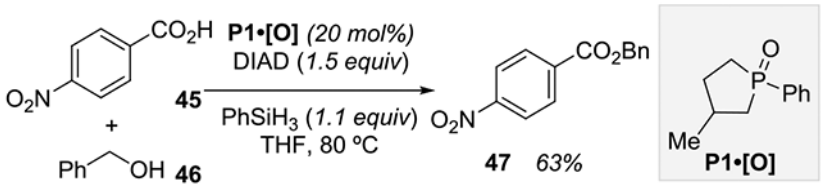

Figure 16.
Phospholane-catalyzed Mitsunobu-type reaction.

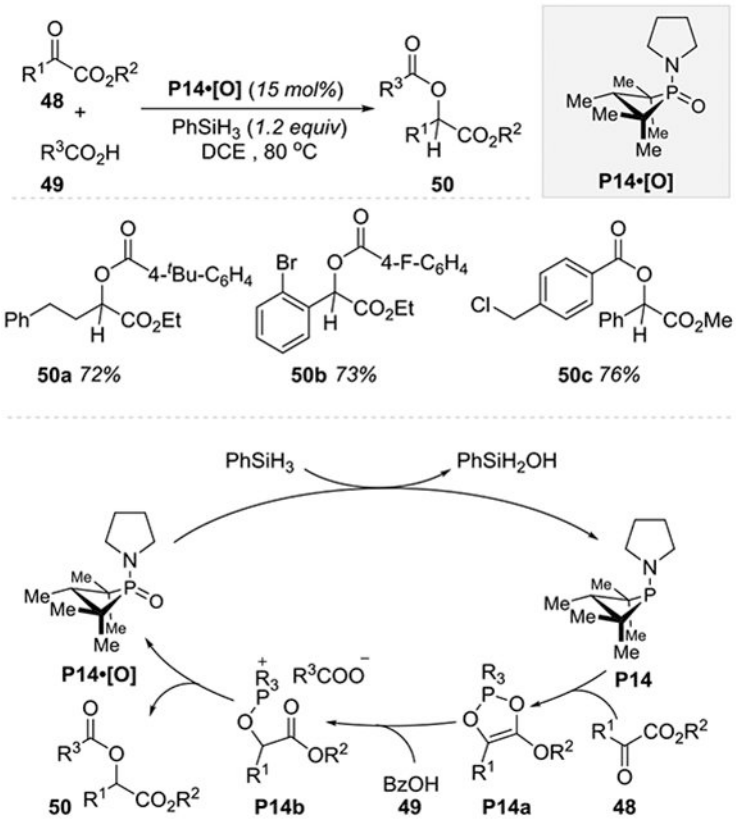

Figure 17.

P^{III}/P^{V}=O catalyzed deoxygenative condensation of α-keto esters with carboxylic acids.

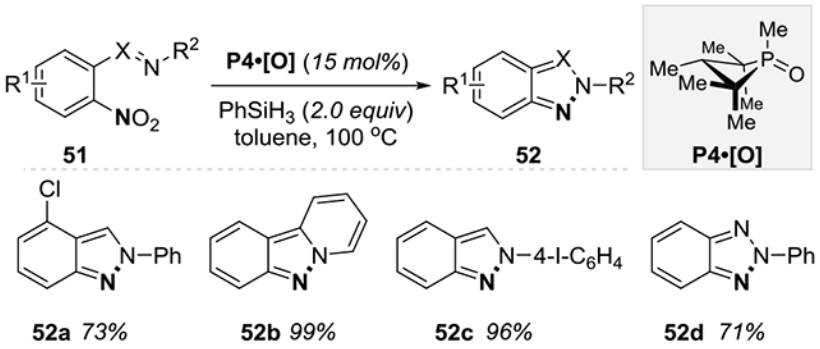

Figure 18.

Biphilic phosphetane-catalyzed N–N bond-forming Cadogan heterocyclization via P^{III}/P^{V}=O redox cycling.

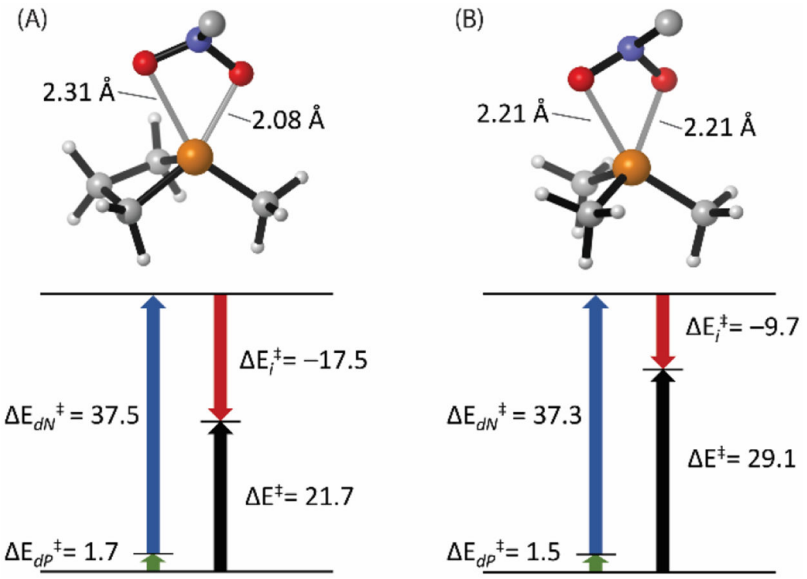

Figure 19.

Transition structures and distortion/interaction analyses for (3+1) transition states (M06-2X/6-311++g(d,p)): (A) phosphetane TS and (B) Me_3P TS. Phosphine distortion energy ($\Delta E_{dP}^{‡}$) in green, nitromethane distortion energy ($\Delta E_{dN}^{‡}$) in blue, fragment interaction energy ($\Delta E_i^{‡}$) in red, activation energy ($\Delta E^{‡}$) in black. All energies in kcal/mol without zero-point correction.

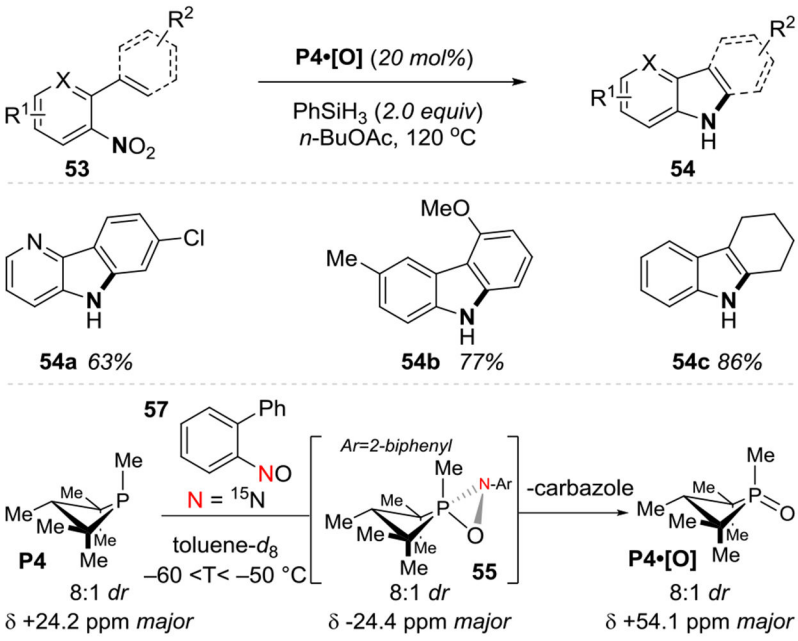

Figure 20.

Biphilic organophosphorus-catalyzed intramolecular $C_{sp}{}^2$-H amination and identification of oxazaphosphirane intermediate.

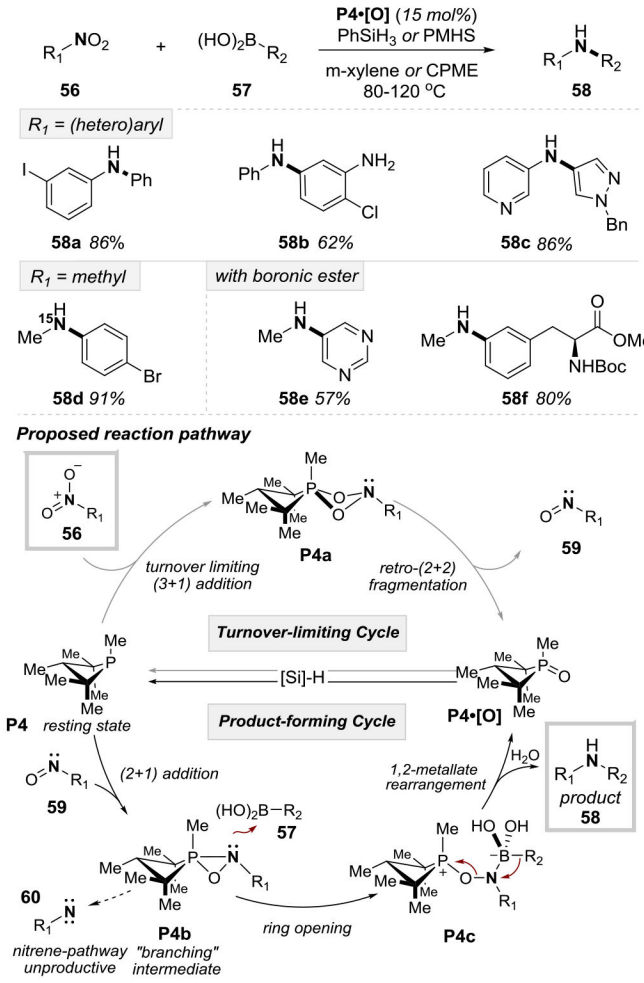

Figure 21.

P^{III}/P^{V}=O catalyzed intermolecular reductive C–N cross coupling of nitroarenes and boronic acids. Boc = *tert*-butyloxycarbonyl.

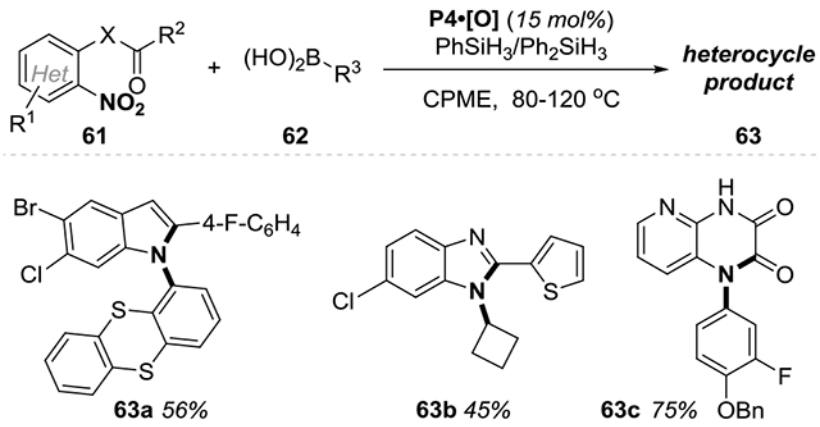

Figure 22.
P^{III}/P^{V}=O-catalyzed cascade synthesis of *N*-functionalized azaheterocycles.

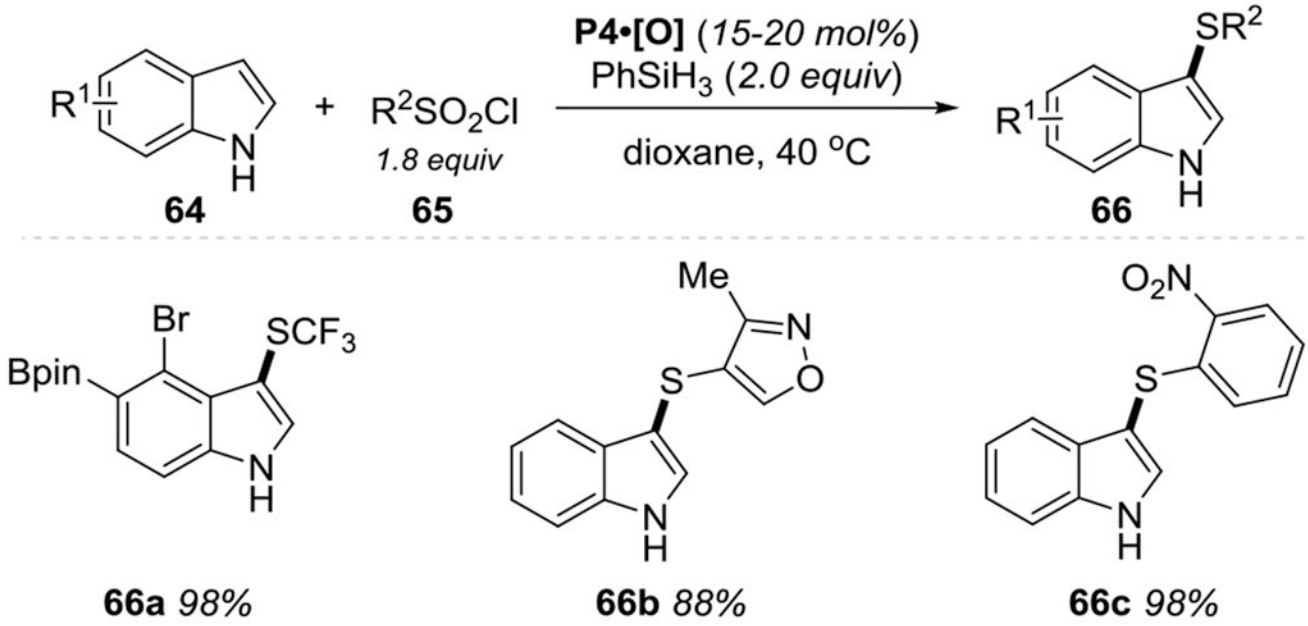

Figure 23.

Phosphetane-catalyzed (fluoroalkyl)sulfenylation via deoxygenation of sulfonyl chlorides. Pin = pinacol.

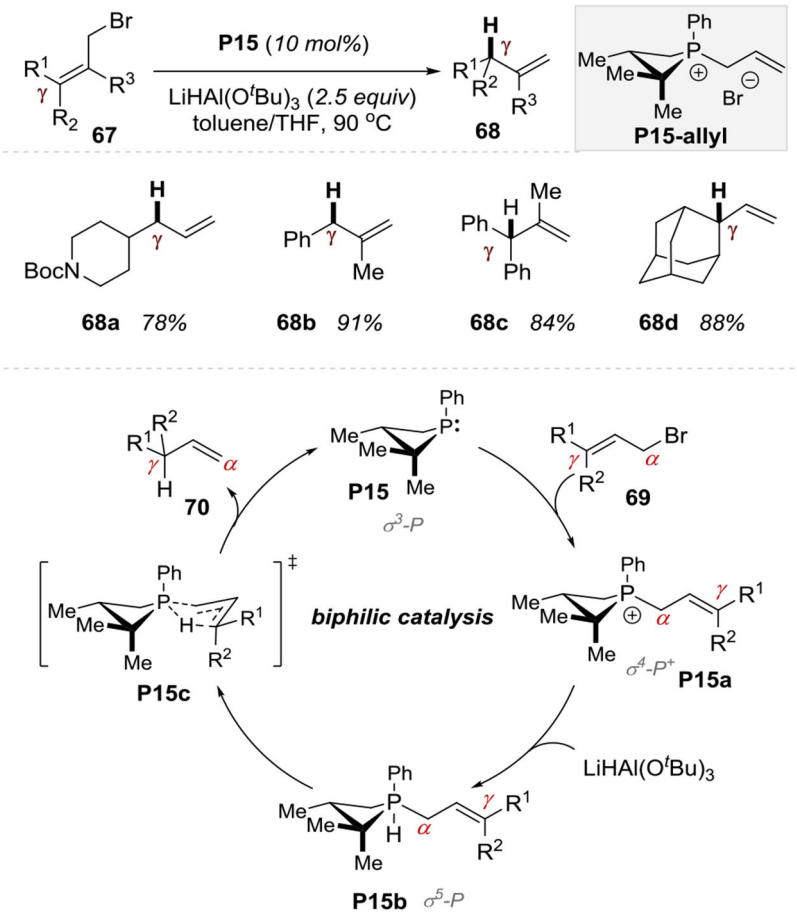

Figure 24.
Organophosphorus-catalyzed regioselective reductive transposition of allylic bromides.

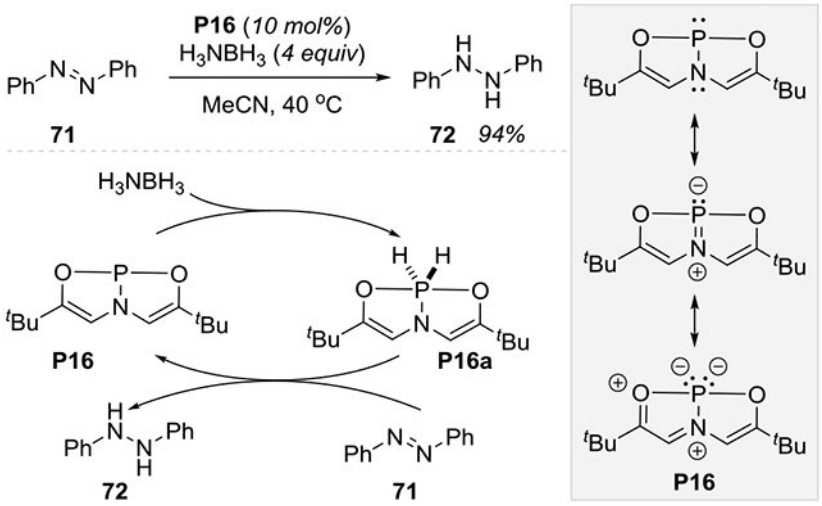

Figure 25.
P^{III}/P^{V}-catalyzed transfer hydrogenation of azobenzene.

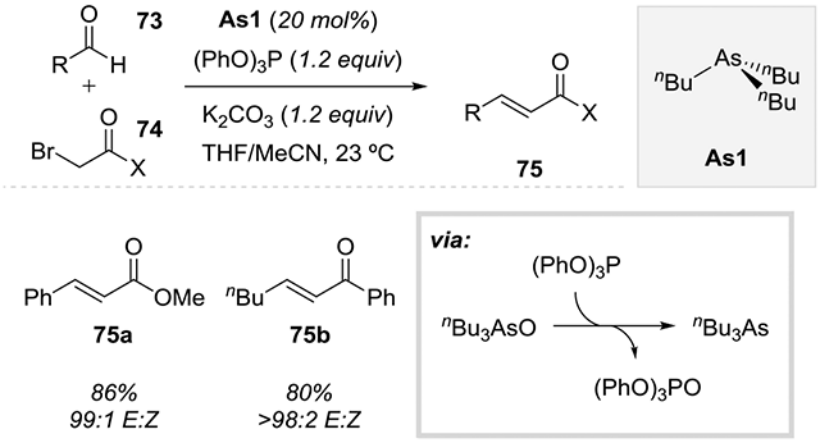

Figure 26.

Organoarsine-catalyzed Wittig reaction employing triphenylphosphite as stoichiometric *O*-atom acceptor.

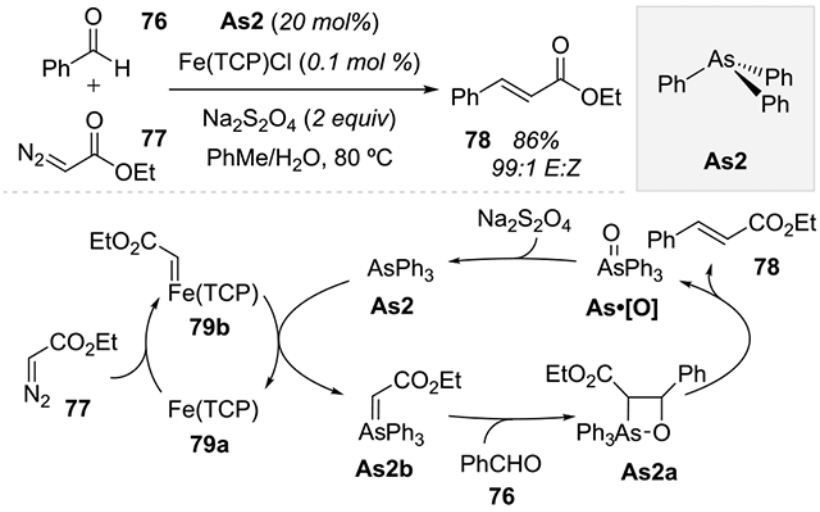

Figure 27.

Organoarsine-catalyzed Wittig-type olefination of aldehydes with diazo compounds, with Fe-porphyrin co-catalyst to facilitate carbene transfer. TCP = tetra(*para*-chlorophenyl)porphyrinate.

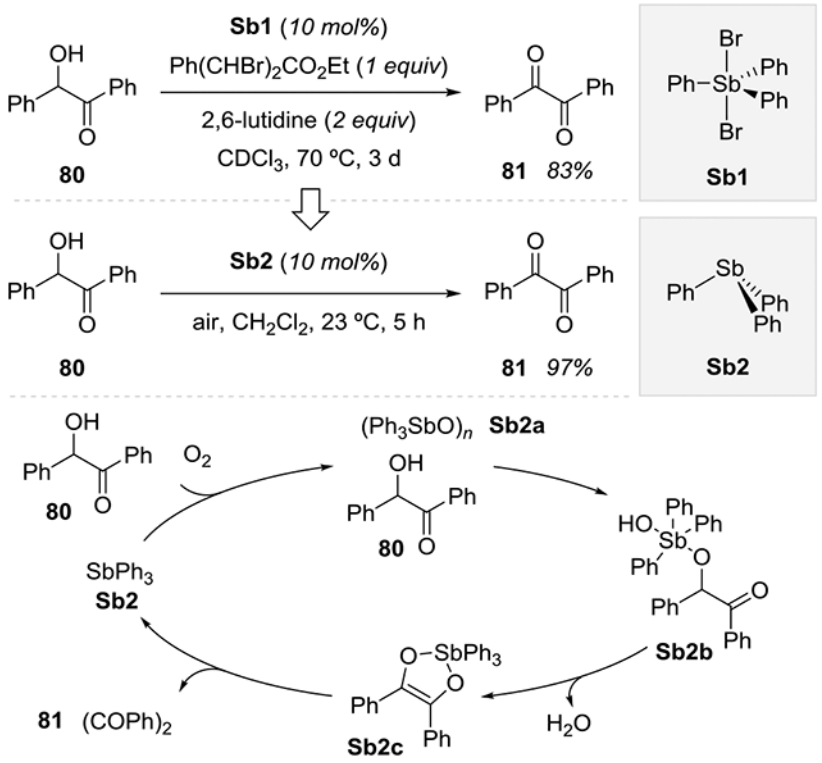

Figure 28.
Benzoin oxidation via organoantimony redox catalysis.

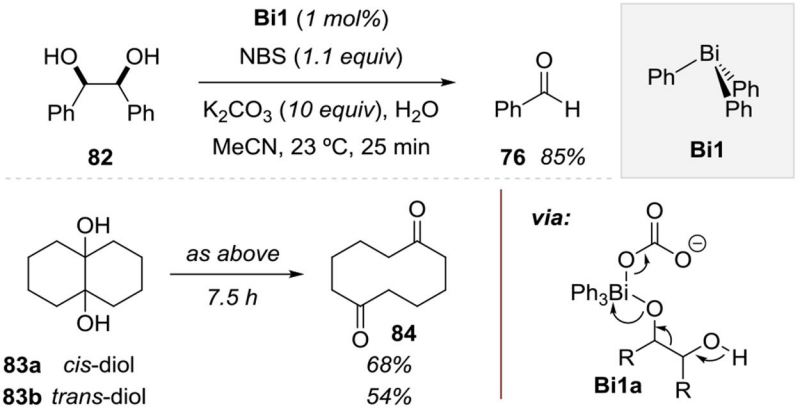

Figure 29.

$BiPh_3$-catalyzed α-glycol cleavage via Bi(V) oxidation. NBS = *N*-bromosuccinimide.

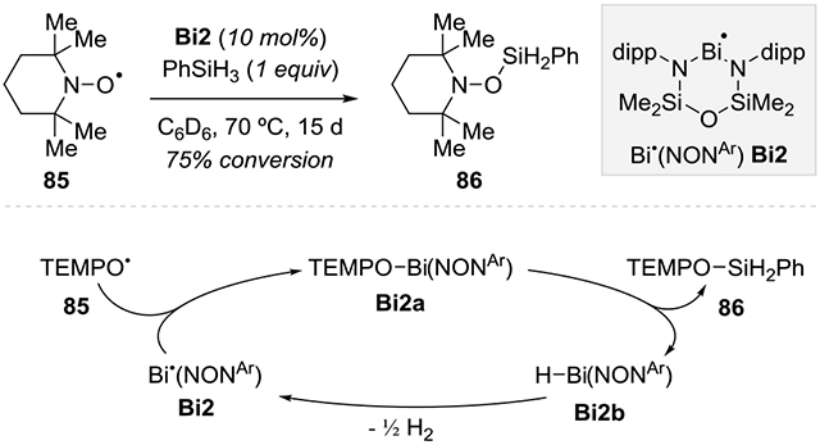

Figure 30.

Bi^{II}/Bi^{III}-catalyzed dehydrogenative O–Si bond formation. Dipp = 2,6-di-*iso*-propylphenyl.

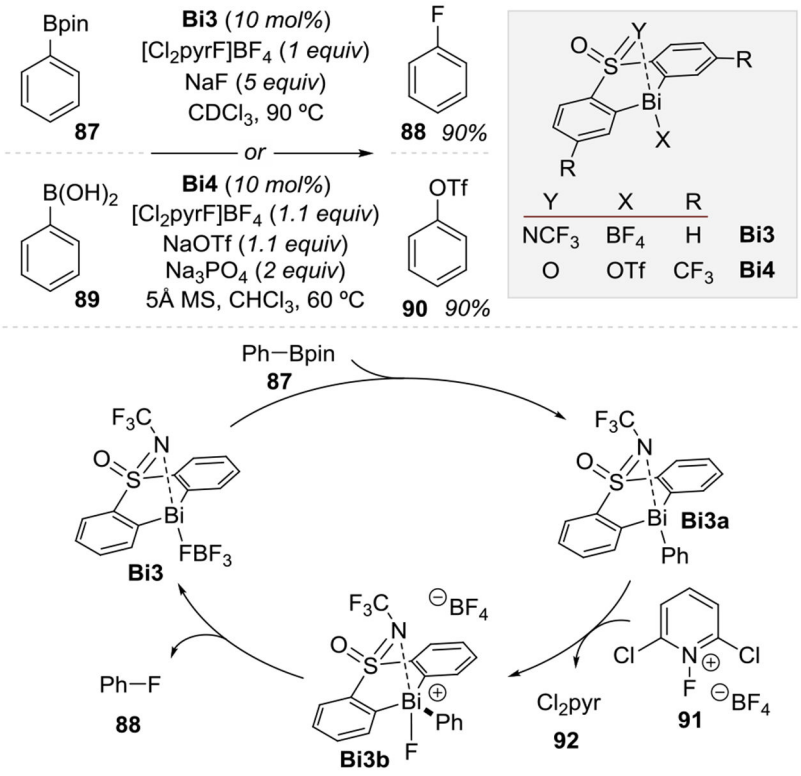

Figure 31.

Bi-catalyzed fluorination and triflation of aryl boronic esters and acids, respectively. Proposed mechanism of fluorination. Tf = triflyl.

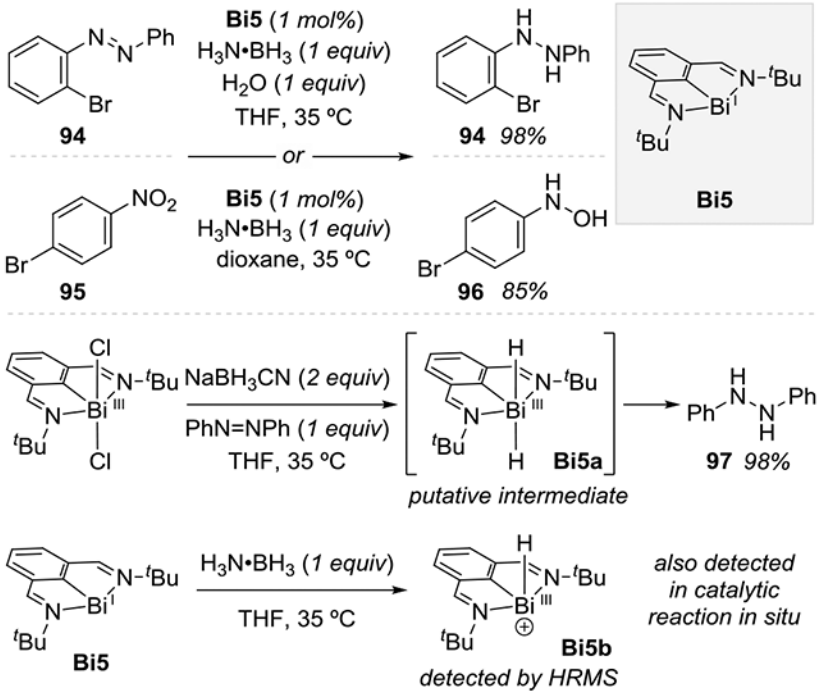

Figure 32.

Bismuthinidene-catalyzed transfer hydrogenation of azoarenes and nitroarenes to hydrazines and hydroxylamines, respectively, with ammonia borane.

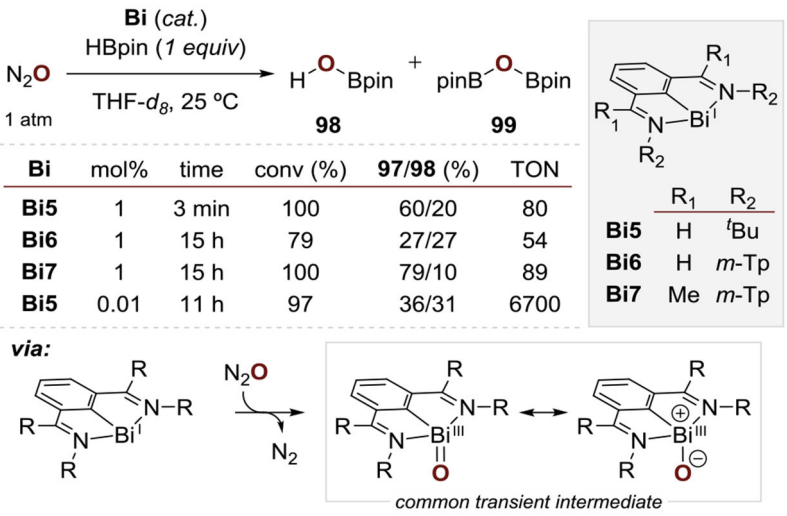

Figure 33.

Bismuthinidene-catalyzed reductive deoxygenation of N_2O via the intermediacy of Bi(III)-oxide equivalents with pinacolborane. *m*-Tp = *meta*-terphenyl.